USGS
science for a changing world

Estimates of Peak Discharge for 21 Sites in the Front Range in Colorado in Response to Extreme Rainfall in September 2013

Scientific Investigations Report 2016–5003

U.S. Department of the Interior
U.S. Geological Survey

Cover photograph. Floodwater was still spilling out from Twomile Creek onto Linden Avenue on September 15, 2013, in North Boulder, Colorado. The effects of several landslide/debris flows generated by saturated conditions during the night of September 11–12 can be seen on Dakota Ridge near the center of the photograph.

Estimates of Peak Discharge for 21 Sites in the Front Range in Colorado in Response to Extreme Rainfall in September 2013

By John A. Moody

Scientific Investigations Report 2016–5003

U.S. Department of the Interior
U.S. Geological Survey

U.S. Department of the Interior
SALLY JEWELL, Secretary

U.S. Geological Survey
Suzette M. Kimball, Director

U.S. Geological Survey, Reston, Virginia: 2016

For more information on the USGS—the Federal source for science about the Earth, its natural and living resources, natural hazards, and the environment—visit http://www.usgs.gov or call 1–888–ASK–USGS.

For an overview of USGS information products, including maps, imagery, and publications, visit http://www.usgs.gov/pubprod/.

Suggested citation:
Moody, J.A., 2016, Estimates of peak flood discharge for 21 sites in the Front Range in Colorado in response to extreme rainfall in September 2013: U.S. Geological Survey Scientific Investigations Report 2016–5003, 64 p., http://dx.doi.org/10.3133/sir20165003.

ISSN 2328-0328 (online)

Contents

Figures

Tables

Conversion Factors

International System of Units to Inch/Pound

Multiply	By	To obtain
	Length	
millimeter (mm)	0.03937	inch (in.)
meter (m)	3.281	foot (ft)
kilometer (km)	0.6214	mile (mi)
kilometer (km)	0.5400	mile, nautical (nmi)
meter (m)	1.094	yard (yd)
	Area	
square kilometer (km^2)	247.1	acre
square kilometer (km^2)	0.3861	square mile (mi^2)
	Flow rate	
cubic meter per second ($m^3\ s^{-1}$)	70.07	acre-foot per day (acre-ft d^{-1})
meter per second (m s^{-1})	3.281	foot per second (ft s^{-1})
cubic meter per second ($m^3\ s^{-1}$)	35.31	cubic foot per second ($ft^3\ s^{-1}$)
cubic meter per second per square kilometer ($m^3\ s^{-1}\ km^{-2}$)	91.49	cubic foot per second per square mile ($ft^3\ s^{-1}\ mi^{-2}$)
liter per second (L s^{-1})	15.85	gallon per minute (gal min^{-1})
cubic meter per second ($m^3\ s^{-1}$)	22.83	million gallons per day (Mgal d^{-1})
millimeter per hour (mm h^{-1})	.03937	inch per hour (in h^{-1})
kilogram per meter per second (kg $m^{-1}\ s^{-1}$)	.055997	pound per inch per second (lb $in^{-1}\ s^{-1}$)
	Acceleration	
meter per square second (m s^{-2})	39.37	inch per square second (in s^{-2})
	Mass	
kilogram (kg)	2.2046	pound (lb)
	Mass flux	
kilogram per meter per second (kg $m^{-1}\ s^{-1}$)	0.6720	pounds per foot per second (lb $ft^{-1}\ s^{-1}$)

Datums

Vertical coordinate information is referenced to the North American Vertical Datum of 1988 (NAVD 88).

Horizontal coordinate information is referenced to the North American Datum of 1983 (NAD 83).

Elevation, as used in this report, refers to distance above the vertical datum.

Supplemental Information

Manning's flow resistance is given in meters to the minus one-third power times seconds ($m^{-1/3}\ s$).

Time is given in hours (h), minutes (min), or seconds (s).

Estimates of Peak Discharge for 21 Sites in the Front Range in Colorado in Response to Extreme Rainfall in September 2013

By John A. Moody

Abstract

Extreme rainfall in September 2013 caused destructive floods in part of the Front Range in Boulder County, Colorado. Erosion from these floods cut roads and isolated mountain communities for several weeks, and large volumes of eroded sediment were deposited downstream, which caused further damage of property and infrastructures. Estimates of peak discharge for these floods and the associated rainfall characteristics will aid land and emergency managers in the future. Several methods (an ensemble) were used to estimate peak discharge at 21 measurement sites, and the ensemble average and standard deviation provided a final estimate of peak discharge and its uncertainty. Because of the substantial erosion and deposition of sediment, an additional estimate of peak discharge was made based on the flow resistance caused by sediment transport effects.

Although the synoptic-scale rainfall was extreme (annual exceedance probability greater than 1,000 years, about 450 millimeters in 7 days) for these mountains, the resulting peak discharges were not. Ensemble average peak discharges per unit drainage area (unit peak discharge, [Q_u]) for the floods were 1–2 orders of magnitude less than those for the maximum worldwide floods with similar drainage areas and had a wide range of values (0.21–16.2 cubic meters per second per square kilometer [$m^3 s^{-1} km^{-2}$]). One possible explanation for these differences was that the band of high-accumulation, high-intensity rainfall was narrow (about 50 kilometers wide), oriented nearly perpendicular to the predominant drainage pattern of the mountains, and therefore entire drainage areas were not subjected to the same range of extreme rainfall. A linear relation (coefficient of determination [R^2]=0.69) between Q_u and the rainfall intensity (I_{Tc}, computed for a time interval equal to the time-of-concentration for the drainage area upstream from each site), had the form: $Q_u=0.26(I_{Tc}-8.6)$, where the coefficient 0.26 can be considered to be an area-averaged peak runoff coefficient for the September 2013 rain storms in Boulder County, and the 8.6 millimeters per hour to be the rainfall intensity corresponding to a soil moisture threshold that controls the soil infiltration rate. Peak discharge estimates based on the sediment transport effects were generally less than the ensemble average and indicated that sediment transport may be a mechanism that limits velocities in these types of mountain streams such that the Froude number fluctuates about 1 suggesting that this type of floodflow can be approximated as critical flow.

Introduction

Floods in the Front Range in Boulder County, Colorado (hereinafter referred to as Colorado Front Range) are generally associated with snowmelt runoff in the spring and early summer months. Numerous regional-regression equations have been developed to estimate peak discharges in ungaged watersheds (Capesius and Stephens, 2009 and references therein). Variables used in these regional-regression equations are typically drainage area, mean watershed slope, and mean annual precipitation; thus, these regional-regression equations are not necessarily suited for estimating peak discharges associated with extreme rainfall and especially extreme rainfall in September when mountain streams are typically at their lowest discharge near the end of the water year (October through September of the following year). The rainfall pattern that developed in September 2013 over the Colorado Front Range was unusual because rainfall intensities were not especially high, but the duration was long for this region (from September 9 to 16). This long duration produced total rainfall exceeding 450 millimeters (mm) at some locations (Gochis and others, 2014).

The extreme rainfall that caused the floods in the mountains was a macro- or synoptic-scale event (1,000 to 1,000,000 square kilometers [km^2]; Hirschboeck, 1988) having a relatively narrow band of rainfall (about [≈] 50 kilometers [km] wide) extending 80–100 km from Golden, Colorado, southeast-to-northwest through Estes Park, Colo., near the Continental Divide almost to the Colorado-Wyoming border (fig. 1). One unusual characteristic of this rainfall was the persistence of the circulation pattern caused by an upper-level ridge to the north in the Canadian Rockies blocking movement and a slow-moving, low-pressure system that "pumped " unseasonable high monsoonal tropical moisture

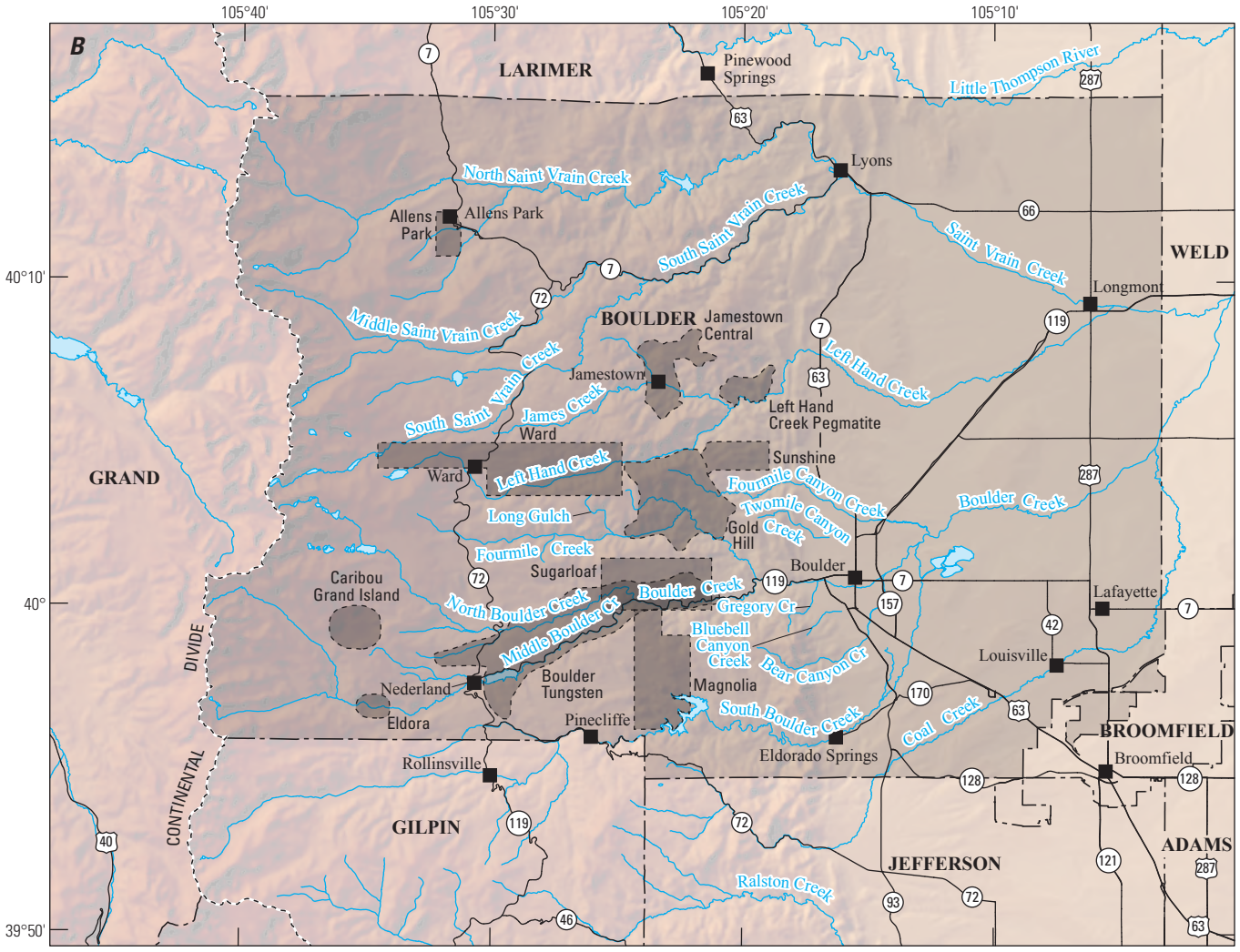

Base from U.S. Geological Survey, The National Map
digital data, 1:1,000,000, 2015
Universal Transverse Mercator, Zone 13N
North American Datum of 1983

0 2 4 6 8 10 MILES
0 2 4 6 8 10 KILOMETERS

Mining districts from http://coloradogeologicalsurvey.org/mineral-resources/historic-mining-districts/boulder-county/

EXPLANATION

- Study area
- Mineral district
- Eldora — Mineral district boundary and identifier

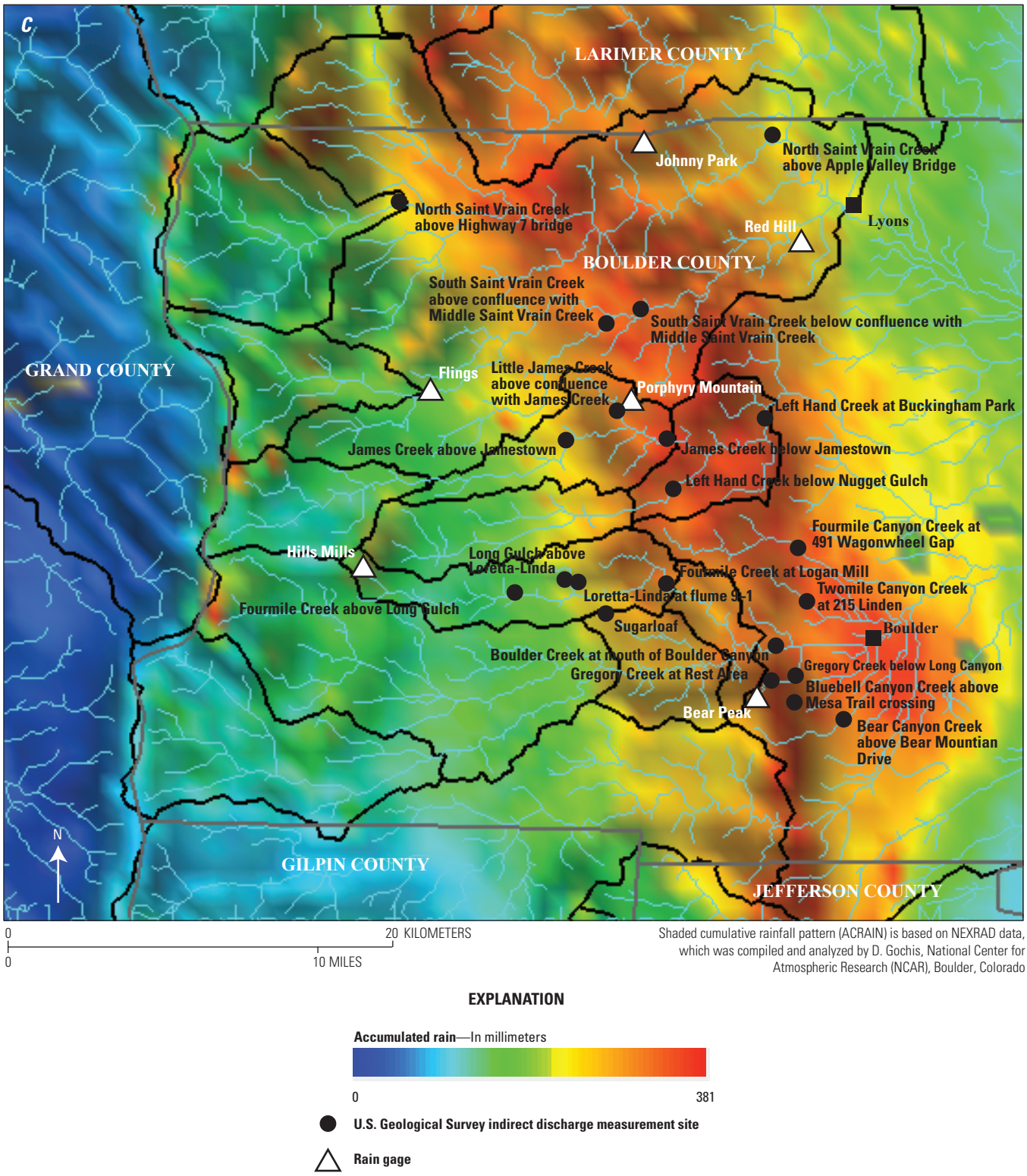

Figure 1. Location of the Front Range, study area, indirect measurement sites, and rain gages. *A*, Front Range relative to the Pacific Ocean. *B*, Part of the Front Range, the study area, and some of the major streams in northern Colorado. *C*, Location of 21 U.S. Geological Survey indirect discharge measurement sites, 6 rain gages, and accumulative rainfall from September 9–16, 2013, in Boulder County, Colorado.

off the Pacific Ocean up against the Colorado Front Range (Lukas, 2013; Gochis and others, 2014). Precipitable water was 36.8 mm, which was greater than the 64-year average maximum for Denver, Colo. (31.2 mm). Estimates by the National Oceanic and Atmospheric Administration of the annual exceedance probabilities for 24 hours (h), 48 h, and 7 days were all greater than 1,000 years (National Oceanic and Atmospheric Administration, 2013) for a narrower band (about 20 km wide, which is essentially the yellow-red band or about 220–380 mm in fig. 1*C*) centered within the larger band extending across Boulder County, Colo. (fig. 1*C*). Soils were probably saturated or near saturation (Gochis and others, 2014) by sunset on September 11, 2013, when 50–100 mm of rain had already fallen (fig. 2). Debris flows (see cover photograph) began as discrete slides of colluvial soil and were initiated when the minimum antecedent rainfall was about 75 mm (Coe and others, 2014). Saturation was measured in south-facing soils (just north of Sugarloaf, fig. 1*B*) just before 0100 h on September 12, 2013 (Ebel and others, 2015), to the west of areas with maximum accumulated rainfall and intensity. After sunset, there was a rapid increase in rainfall, and most mountain streams peaked during the nighttime hours.

Flood conditions in steep, narrow, and rough mountain channels differ from sand-bed streams with wide flood plains that are more typical of lower elevations. Generally, in these mountain channels, slopes (S, nondimensional), are greater than 0.01, and the size of bed and bank roughness elements (that is, D_{84}, in millimeters, is the roughness diameter for which 84 percent of the elements are smaller) are greater than 32 mm. In general, the mountain streams measured in this report have narrow flood plains such that conveyance in the channel is usually greater than over the flood plain. Although the bed and banks of mountain streams are rough in the absolute sense, what is important in all flows is the relative submergence (equal to the ratio of the hydraulic radius [R], in millimeters, to D_{84}). For step-pool types of mountain streams R/D_{84} is often less than (<) 1 (Aberle and Smart, 2003; Wilcox and others, 2006; Comiti and others, 2007; Yochum and Bledsoe, 2010; Yochum and others, 2012), and most discharge measurements in other types of mountain streams (Barnes, 1967; Judd and Peterson, 1969; Limerinos, 1970; Bathurst, 1978, 1985; Griffiths, 1981; Marchard and others, 1984; Jarrett, 1984; Hicks and Mason, 1998) have been made for relatively low water conditions such that R/D_{84} is frequently <1;

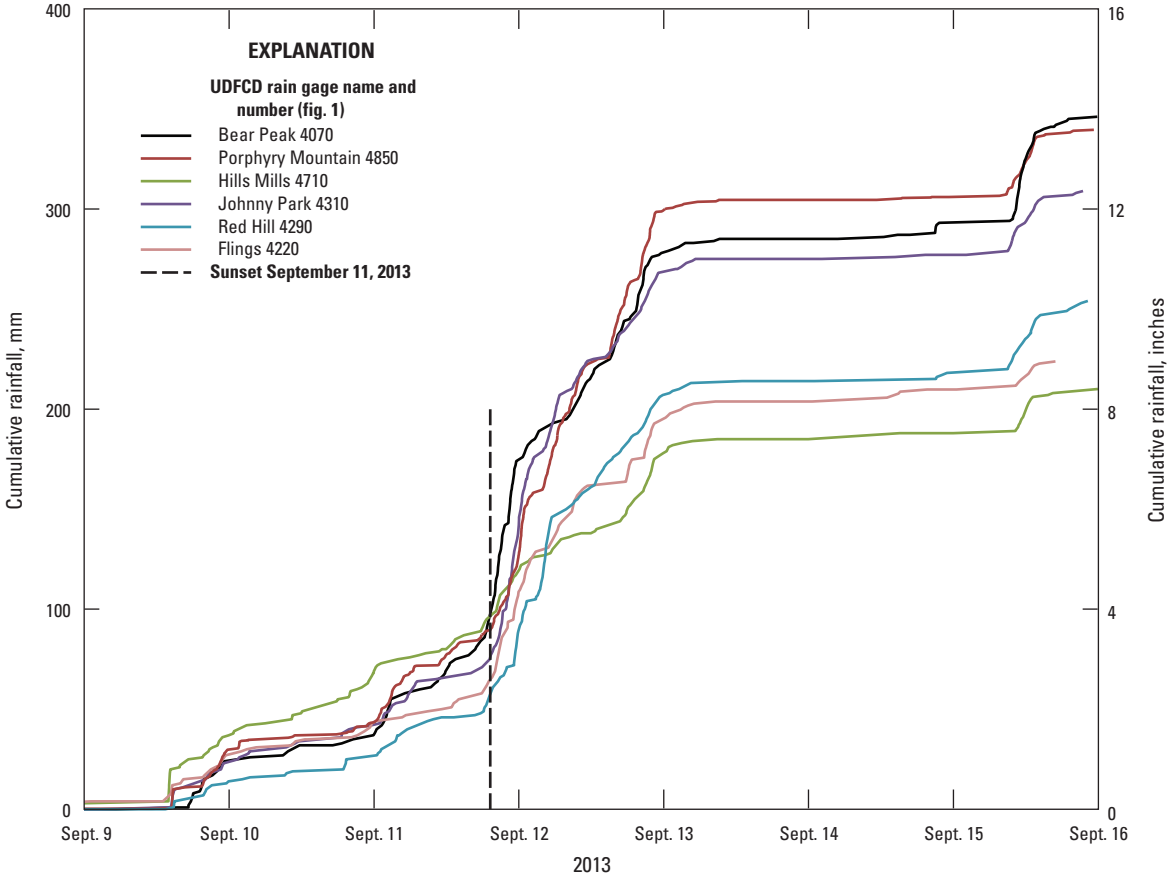

Figure 2. Cumulative rainfall for select Urban Drainage and Flood Control District (UDFCD) rain gages during September 9–16, 2013, along the Front Range in Boulder County, Colorado. Most soils were probably saturated by sunset (1916 Mountain Daylight Time [MDT]), and water discharge is estimated to have peaked between 2100 and 2400 MDT on September 11, 2013.

however, for floodflows, R/D_{84} can be greater than (>) 1. Even so, the surface water is generally turbulent caused by the large submerged roughness elements and irregular banks (fig. 3). Water surging up and down the banks makes estimating high-water elevations difficult, and estimates can vary substantially across the channel.

Purpose and Scope

This report presents estimates of peak discharge of the September 2013 floods at 21 mountain sites in the Colorado Front Range based on indirect measurements. These sites are limited to Boulder County, Colo., and were selected to represent a range of contributing area (0.0084–337 km^2). Several different methods are used, and an ensemble average and coefficient of variation (COV) provides a mean value and an estimate of the uncertainty of the mean value. In addition, estimates of the average peak rain intensity are calculated for the contributing area upstream from each site to determine a possible relation between the driver, rainfall intensity, and the response, peak flood discharge, (see the "Field Methods" section for further explanation). This flood response to the extreme rainfall is compared with historical and worldwide extraordinary floods to give emergency managers a context for interpreting the September 2013 floods, which caused some deaths and evacuations and isolated some mountain communities for weeks to months (Lukas, 2013).

Description of Study Area

The Colorado Front Range in Boulder County rises abruptly from the Great Plains along a north-south trending line. The base of the mountain range begins at about 1,650 meters (m) and the top of the mountain range culminates along the north-south trending Continental Divide (at about 3,650 m) in a distance of only about 32 km (Bilodeau and others, 1987). This situation creates a steep mountain front that affects the weather (snow accumulation and rainfall intensity and duration). The Colorado Front Range is in the interior of North America (fig. 1*A*), and has a semiarid, continental climate. Peak rainfall is generally in April and May from low intensity (<25 millimeters per hour [mm h^{-1}]), long duration (hours to days) cyclonic storms. A secondary peak in July or August (Hansen and others, 1978) is usually associated with high-intensity (>25 mm h^{-1}), short duration (1–2 h) convective storms during the North American monsoon season from June to September (Douglas and others, 2004). Mean precipitation for the 6 months from April through September ranges from about 330 mm at the base of the mountains to 430 mm near the Continental Divide (Hansen and others, 1978). This stretch of the Colorado Front Range is dissected by several streams (fig. 1*B*) that originate along the Continental Divide and generally flow west to east out of the mountains onto the Great Plains. The headwaters and major segments of drainage basins are in predominantly Precambrian crystalline bedrock

Figure 3. Turbulent flow in James Creek through Jamestown, Colorado, on September 12, 2013. View is downstream after peak flow showing how surface waves create uncertainty in the actual elevation of the high-water marks along creek banks. Photograph taken by Mark Williams.

(granites, gneisses, and granodiorites, Bilodeau and others, 1988; Birkland and others, 2003), and the streams only pass through a short (2–5 km) segment of sedimentary bedrock as they exit the mountain front. Soils derived from these bedrocks form "a thin mantle of residual regolith", which are only "a few centimeters to 1–2 m in thickness" (Bilodeau and others, 1987, p. 305; Moreland and Moreland, 1975; Jarrett and Costa, 2006).

Population of Boulder County in 2014 was about 313,000 people with about 58,000 people living in the mountains (http://quickfacts.census.gov/qfd/states/08/08013.html, accessed November 2015). County roads and highways follow narrow canyons and provide critical access to mountain towns and communities (Allens Park, Jamestown, Lyons, Nederland, Ward, and Sugarloaf; see fig. 1*B*). Most of these were founded during the gold rush (1859–early 1860s) in and near the crystalline bedrock region, which was the source of gold and other minerals (fig. 1*B*). These roads and highways were thought to be most susceptible to summer floods during the North American Monsoon season when large convective storms commonly develop and sometimes stall over the areas of uplift provided by the Colorado Front Range. Most notably was the catastrophic summer flood (July 31, 1976) on the Big Thompson River caused by a stationary convective storm (about 190 mm h^{-1}, Jarrett and Costa, 2006). This flood caused over $35 million in damages (1977 dollars), claimed the lives of 144 people, forced the evacuation of about 800 people by helicopter, and raised the public awareness of summer floods (Jarrett and Costa, 2006). Meteorological conditions conducive to these numerous summer floods during the Monsoon season are less predictable than the annual floods from snowmelt runoff, but are now more predictable than the rare meteorological conditions that produced the September 2013 floods. Many people living in the Colorado Front Range area did not expect the magnitude of these floods, and many were evacuated by helicopter from mountain towns.

Field Methods

Indirect measurement sites were selected after damaged roads were repaired and reopened. Road repair and the onset of winter prolonged the field data collection. Sites were relatively straight reaches without significant expansion and minimal evidence of deposition. The deposition was important because it was assumed that erosion and scour of the channel was on the rising limb of the flood so that the measured cross-sectional area represented the area at peak discharge. Measurement reaches were on the order of 10 stream widths long with minimal erosion along the banks of the reach. Cross sections were established perpendicular to the estimated flow direction and approximately one stream width apart. High-water elevations were flagged, in some cases, months before the cross sections were surveyed when high-water indicators were undisturbed knowing that winter weather might destroy some indicators. Elevations were measured (using a metric rod and survey level; NAK2, Wild Heerbrugg Instrument) at stations from the left-bank, high-water mark along a steel tagline stretched across the channel to the right-bank, high-water mark. Left and right refers to looking downstream. This method can measure repeat cross-sectional elevations with an average elevation error of 0.014–0.019 m (Moody and Meade, 1990). The uncertainty in the elevation of the high-water marks varied and was estimated to be on the order of plus or minus (±) 0.1 m based on field observations of turbulent water surfaces. Typical maximum water depths were 1–2 m, so the uncertainty in the high-water elevations themselves could introduce an uncertainty of the discharge on the order of ±10 percent. The highest "debris line" was not necessarily selected as a high-water mark when a band of debris provided some visual clue to the possible range in the undulations of the high-water surface. Other high-water indicators besides debris lines were bent-over vegetation, scour lines, and fine sediment deposition. Left- and right-bank, high-water marks were photographed in addition to downstream, left and right cross-stream, and upstream views. The purpose of these cross-sectional surveys was to determine the cross-sectional area and not the roughness characteristics of the bed and bank surfaces.

The characteristics of the bed and bank roughness elements (that is, boulders, roots, tree boles, and debris) were measured after the cross-sectional measurements. In some cases, this was several months later because streams had frozen. Roughness was measured at grid points determined by stretching a metric tape from the first cross section downstream along the estimated center/thalweg line of the channel and measuring at approximately equal distance intervals in the downstream direction and on either side of the tape. The distance interval was determined by the characteristic size of the roughness elements such that multiple measurements were not made of the same element nor were many roughness elements within one grid cell. In general, grid spacing was either 0.5 or 1 m. Only the protruding height above the bed and the cross-stream diameter of one roughness element (greater than or equal to [≥] 32 mm) within a "search radius" of 0.1 m vertically below a grid point were measured. Those grid points with elements <32 mm were noted as "<32" and included in determining the D_{84} and roughness diameter for which 50 percent of the elements are smaller (D_{50}) at each site. The goal was to measure 100–150 roughness elements. Many roughness elements were too large and embedded into the bed so that they could not be removed to measure all axes. For this reason the protruding height was measured by placing a level on top of the element and measuring the perpendicular distance from the bottom of the level to the bed in contact with the element. In the case of roughness elements in the bank, the distance was measured perpendicular to the general bank surface; thus, it is important to remember that all values of D_{84} and D_{50} reported here correspond to the protrusion height and not the b-axis of the roughness element.

Indirect Discharge Calculations

Several methods (an ensemble) were used to estimate each peak discharge. The ensemble average and standard deviation provide an estimate of the uncertainty of these discharge values. Ensemble averaging has been a technique used in meteorology for creating a forecast based on predictions generated by several independent hydrologic models where each model has its advantages, disadvantages, and associated errors. Ensemble averaging tends to cancel out the errors from each model and, thus, provide a better overall prediction (Ajami and others, 2006).

The primary problem for indirect measurements of discharge made after a flood is to estimate the cross-sectional average velocity, (v, in meters per second [m s^{-1}]) at the time of the peak flood. The product of v times the maximum cross-sectional area, (A, in square meters [m^2]) measured in the field after the floods provides an estimate of the peak discharge, (Q, in cubic meters per second [m^3 s^{-1}]).

$$Q=Av \tag{1}$$

The essence of the problem, therefore, is to select a resistance equation or method that relates v to the hydraulic roughness and other hydraulic variables. One common resistance equation is Manning's equation (Chow, 1964, Benson and Dalrymple, 1967, and Rantz and others, 1982)

$$v = \frac{S^{1/2}R^{2/3}}{n} \tag{2}$$

where n, in meters to the negative one-third power times seconds [$m^{-1/3}$ s] is Manning's roughness coefficient (Barnes, 1967).

For 19 of the 21 sites, 5 methods were selected: Cowan, Jarrett, Empirical, Critical flow, and the Slope-area method. These are independent methods for calculating the peak discharge in the main channel, which conveys most of the flow; however, each method uses the Cowan method for calculating flow over the adjacent banks and any existing flood plain. For the single measurement site at Bluebell Canyon Creek above the Mesa Trail crossing (table 1), an additional method attributed to Bagnold (Hungr and others, 1984) was included with the previous five methods. For the Sugarloaf measurement site (table 1) with the smallest drainage area (0.0084 km^2), the Measured "n," Yochum, Comiti, and Critical flow methods were used.

An average high-water elevation was computed at each cross section. Initially at the first sites, the quality (good, fair, poor, and very poor) of the left- and right-bank, high-water mark was not recorded, but at later sites the quality was recorded in the field notes. The average high-water elevation was then computed as a weighted average with a higher-quality mark weighted as twice a lower-quality mark. Flow depths were computed as the vertical distance below the weighted-average high-water elevation. A reach-average, water-surface slope (S) was computed by fitting a linear-regression line (Helsel and Hirsch, 2002) through all high-water elevations. Recognizing the uncertainty of the high-water elevations mentioned above, this reach-average, water-surface slope was used for computing the peak discharge estimate at each cross section, rather than using the local slopes at each cross section. The peak discharge estimate for each method was the average of the discharges at each cross section. The ensemble average was the average of the estimated peak discharge for each method, and the uncertainty was the COV of the estimated peak discharges.

Cowan Method

The Cowan method, originally proposed by Cowan (1956), assumes that the total resistance characterized by Manning's roughness coefficient, n ($m^{-1/3}$ s) is a simple linear sum of the following effects: (1) irregularities of the bed and bank surfaces, (2) variation in the shape and size of the channel cross section, (3) obstructions, (4) vegetation, and (5) channel meandering. Cowan's original publication has been expanded, and more extensive tables have been published for determining Manning's n for flood-plain surfaces and main channels (Arcement and Schneider, 1992). After surveying the cross sections and before applying any other method, values of Manning's n were selected (using Arcement and Schneider, 1992) for each increment of width in the cross section from the left-bank to the right-bank, based on high-water marks and photographs taken at each cross section.

Jarrett Method

The Jarrett method uses an empirical relation based on data collected from 21 sites on mountain streams in Colorado with channel slopes ranging from 0.002 to 0.04 (Jarrett, 1984). Manning's n is only a function of the friction slope (which can be estimated by water-surface slope) and hydraulic radius because "as slope increases, finer material is removed and larger particles remain in the channel" (Jarrett, 1987, p. 57). The relation (using metric units) is:

$$n = 0.322S^{0.38}R^{-0.16}, \tag{3}$$

which is applicable to the main channel but not adjacent flood plains; thus, this relation was applied to each increment of width in the main channel, and the values of n determined by the Cowan method were used for the adjacent flood plains.

Table 1. Site characteristics, indirect peak discharge estimates, and peak runoff coefficients for the September 2013 floods in the mountains of Boulder County, Colorado.

[NAD 83, North American Datum of 1983; km^2, square kilometers; m, meter; D_{50}, roughness diameter for which 50 percent of the elements are smaller; mm, millimeters; D_{84}, roughness diameter for which 84 percent of the elements are smaller; $m^3\ s^{-1}$, cubic meters per second; COV, coefficient of variation; $m^3\ s^{-1}\ km^{-2}$, cubic meter per second per square kilometer; min, minutes; and $mm\ h^{-1}$, millimeters per hour; na, not applicable]

Measurement site name	Latitude (NAD 83)	Longitude (NAD 83)	Drainage area (km^2)	Mean water-surface slope	Mean bed slope	Reach averaged hydraulic radius (m)	Width/depth	Bed material			Ensemble average peak discharge ($m^3\ s^{-1}$)	COV	Unit peak discharge ($m^3\ s^{-1}\ km^{-2}$)	Time to concentration, T_c (min)	Average peak rainfall intensity during T_c ($mm\ h^{-1}$)	Peak runoff coefficient
								D_{50} z-axis (mm)	D_{84} z-axis (mm)	D_{84} cross-stream axis (mm)						
Saint Vrain Basin																
North St. Vrain Creek above Highway 7 Bridge	40.21887	-105.52828	85	0.013	0.011	0.7	20.3	62	105	160	18	0.24	0.21	184	6.8	0.11
North St. Vrain Creek above Apple Valley Bridge	40.24795	-105.28990	306	0.011	0.006	1.9	21.0	80	150	300	385	0.21	1.26	506	12.6	0.36
South St. Vrain Creek above confluence with Middle St. Vrain Creek[1]	40.16661	-105.39830	33.4	0.031	0.033	1.1	13.3	190	217	500	66	0.26	1.97	288	14.6	0.49
South St. Vrain Creek below confluence with Middle St. Vrain Creek	40.17041	-105.37823	185	0.019	0.021	1.5	14.6	110	240	500	123	0.22	0.66	326	14.9	0.16
Left Hand Basin																
Little James Creek above confluence with James Creek	40.11698	-105.39265	7.76	0.043	0.043	1.1	12.0	32	150	400	74	0.30	9.5	56.8	24.5	1.4
James Creek above Jamestown[1]	40.11185	-105.40648	64.8	0.070	0.051	1.2	8.1	140	400	800	102	0.40	1.6	122	17.7	0.32
James Creek below Jamestown	40.10831	-105.36801	43.7	0.037	0.036	1.4	12.5	100	217	470	122	0.35	2.8	162	16.7	0.60
Left Hand Creek below Nugget Gulch	40.09005	-105.36046	50.7	0.047	0.049	1.1	10.1	130	380	640	52	0.24	1.0	196	16.6	0.22
Left Hand Creek at Buckingham Park	40.11231	-105.30717	119	0.022	0.018	1.8	12.9	67	173	375	199	0.21	1.7	263	15.5	0.39

Table 1. Site characteristics, indirect peak discharge estimates, and peak runoff coefficients for the September 2013 floods in the mountains of Boulder County, Colorado.—Continued

[NAD 83, North American Datum of 1983; km^2, square kilometers; m, meter; D_{50}, roughness diameter for which 50 percent of the elements are smaller; mm, millimeters; D_{84}, roughness diameter for which 84 percent of the elements are smaller; m^3 s^{-1}, cubic meters per second; COV, coefficient of variation; m^3 s^{-1} km^{-2}, cubic meter per second per square kilometer; min, minutes; and mm h^{-1}, millimeters per hour; na, not applicable]

Measurement site name	Latitude (NAD 83)	Longitude (NAD 83)	Drainage area (km^2)	Mean water-surface slope	Mean bed slope	Reach averaged hydraulic radius (m)	Width/depth	Bed material			Ensemble average peak discharge (m^3 s^{-1})	COV	Unit peak discharge (m^3 s^{-1} km^{-2})	Time to concentration, T_c (min)	Average peak rainfall intensity during T_c (mm h^{-1})	Peak runoff coefficient
								D_{50} z-axis (mm)	D_{84} z-axis (mm)	D_{84} cross-stream axis (mm)						
Boulder Basin																
Fourmile Canyon Creek at 491 Wagonwheel Gap	40.06412	-105.30923	12.5	0.048	0.072	1.07	12.6	110	250	445	75	0.30	6.0	86	35.7	0.61
Twomile Canyon Creek at 215 Linden	40.04284	-105.29832	3.36	0.067	0.071	0.92	3.4	170	500	600	26	0.19	7.7	36	49.0	0.57
Fourmile Creek above Long Gulch	40.03699	-105.45409	22.5	0.033	0.019	0.61	10.2	60	120	260	12	0.38	0.51	105	11.8	0.16
Long Gulch above Loretta-Linda	40.04102	-105.42396	3.59	0.077	0.069	0.61	6.9	69	145	360	16	0.48	4.5	33	27.0	0.59
Loretta-Linda at flume 9-1	40.04022	-105.42127	0.39	0.128	0.12	0.40	6.5	87	140	300	6.3	0.57	16.2	8.2	51.0	1.14
Sugarloaf[2]	40.03215	-105.40255	0.0084	0.366	0.37	0.075	18.3	70	110	250	0.057	0.35	6.8	1.3	45.7	0.53
Fourmile Creek at Logan Mill	40.04210	-105.36481	49.3	0.032	0.019	0.96	15.1	78	190	140	67	0.30	1.4	202	12.9	0.38
Boulder Creek at mouth of Boulder Canyon	40.01215	-105.30373	337	0.028	0.027	1.52	11.8	200	450	700	109	0.17	0.32	443	11.5	0.09
Gregory Creek below Long Canyon	39.99718	-105.29941	2.94	0.099	0.065	0.80	7.2	200	500	900	17	0.43	5.8	22	36.3	0.51
Gregory Creek at Rest Area	39.99718	-105.29296	3.67	0.065	0.073	0.93	10.6	130	240	470	43	0.28	11.7	27	37.5	1.0
Bluebell Canyon Creek above Mesa Trail Crossing	39.98965	-105.28704	0.42	0.153	0.14	0.63	15.4	84	200	550	[3]95	0.26	[3]226	9.2	38.0	na
Bear Canyon Creek above Bear Mountain Drive	39.97243	-105.27144	5.69	0.055	0.056	1.92	5.8	40	710	130	12	0.49	2.1	52	32.1	0.24

[1]The upper South St. Vrain Creek is diverted into James Creek so that 42.8 km^2 has been added to the drainage area of James Creek above Jamestown and 42.8 km^2 subtracted from the drainage area of the South St. Vrain above confluence with Middle St. Vrain Creek.

[2]The last two downhill cross sections at Sugarloaf site had distinctly different peak discharge estimates than the upper six cross sections (see table 16). No obvious tributary was seen between the upper six and lower two cross sections. Using all eight cross sections gives an ensemble average of 0.12 m^3 s^{-1} with COV of 0.33 and a physically unrealistic runoff coefficient of 1.1.

[3]It is believed that the "flood" in Bluebell Canyon Creek was a debris flow.

Empirical Method

The variable-power law form of the resistance equation proposed by Ferguson (2007) includes deep flow (first term, $R/D_{84}>4$) and shallow flow (second term, $R/D_{84}<4$) conditions:

$$n = \frac{R^{1/6}}{g^{1/2}}\left[\frac{1}{c_1^2\left(\frac{R}{D_{84}}\right)^{1/3}} + \frac{1}{c_2^2\left(\frac{R}{D_{84}}\right)^{2}}\right]^{1/2}, \quad (4)$$

where g, in meters per square second (m s^{-2}) is the acceleration of gravity. Typical values of the dimensionless regression coefficients, c_1 and c_2 (given by Ferguson, 2007) range from 6.1 to 7.3 for c_1 and from 2.3 to 2.5 for c_2. The range of c_1 and c_2 values is a result of using different datasets. For the peak discharge measurement reported here, a group of 13 existing datasets was selected from published literature (Barnes, 1967; Bathurst, 1985; Griffiths, 1981; Hicks and Mason, 1998; Jarrett, 1984; Judd and Peterson, 1969; Kean and Smith, 2010; Limerinos, 1970; Marchard and others, 1984; Pitlick, 1992), which had conditions similar to the streams measured in this report ($0.0055<S<0.37$; 0.075 m$<R<$1.9 m; 105 mm $<D_{84}$ [protruding height]$<$ 710 mm; and $1.5<R/D_{84}<30$).

The values of Manning's n estimated by using equation 4 were compared with the measured values. Parameters, c_1 and c_2, were varied to minimize the coefficient of determination (R^2) for the linear regression of the residuals (measured n minus estimated n versus measured n) and the root mean square error (RMSE) (Helsel and Hirsch, 2002). The resulting values were c_1=7.3 and c_2=2.3, which gave an R^2 value of 0.19 for the residuals and a RMSE of 0.016 m$^{-1/3}$ s (fig. 4). Equation 4, with c_1=7.3 and c_2=2.3, was applied to each increment of width in the main channel, and the values of n determined by the Cowan method were used for the adjacent flood plains.

Critical Flow Method

Critical flow assumes the Froude number (ratio of flow velocity to the shallow water wave speed) is 1 (Chow, 1964). The consequence of this assumption is that v simply equals $\sqrt{gh}$, where h (in meters) is the depth, and thus is independent of any roughness coefficient. This approximation has been applied by others for mountain stream (Jarrett, 1984; Grant, 1997; Moody and Martin, 2001b; Yochum and Moore, 2013). Critical flow conditions are not constant in time and space but represent average conditions over time and space.

Slope-Area Method

The slope-area method determines the peak discharge using the slope-area calculation (SAC) program developed by the U.S. Geological Survey (Fulford, 1994). It is based on the one-dimensional, gradually varied, steady flow equations. This multireach computation represents the energy balance over the entire reach, not simply an average of the cross sections defining the reach and can give reliable computations for reaches where the Froude number is greater than about 1.2 (M. Smith, U.S. Geological Survey, oral commun., 2015). The initial SAC run used the Manning's n determined using the Cowan method for the left-bank flood plain, main channel, right-bank flood plain; and the reach-averaged, water-surface slopes. The initial result often indicated a spread (the percent difference between discharge computed with no expansion loss and discharge computed with full expansion loss divided by the discharge computed with full expansion loss) for some reaches between cross sections that were ≥1. Successive runs of the SAC program were made by adjusting the local slope until the spread was reduced to 1 or 0, and the length of the reach over which the spread was <1 was maximized. This final reach was not necessarily the entire reach. The discharge for this reach was recorded as the peak discharge, and the uncertainty was calculated as the standard deviation of the discharges at each cross section in this final reach.

Bagnold Method

During the extreme rainfall of September 2013, it is possible that some flows in mountain channels were debris flows. Several empirical equations have been proposed for estimating velocity of a debris flow (Hungr and others, 1984; Prochaska and others, 2008). Some require measurements of the superelevation in bends, which could not be applied to the "straight" reaches selected for indirect measurements. Other equations gave nonzero values of v when either the slope or flow h were 0, which is not physically realistic; however, one equation attributed to Bagnold (Hungr and others, 1984) was selected because it did not give a nonzero velocity:

$$v = \frac{2}{3}\epsilon h^{3/2} S^{1/2} \quad (5)$$

where ϵ is a dimensional coefficient equal to 3.25 m$^{1/2}$ s^{-1}. This relation was applied to each increment of width in the main channel, and the values of n determined by the Cowan method were used for the adjacent flood plains.

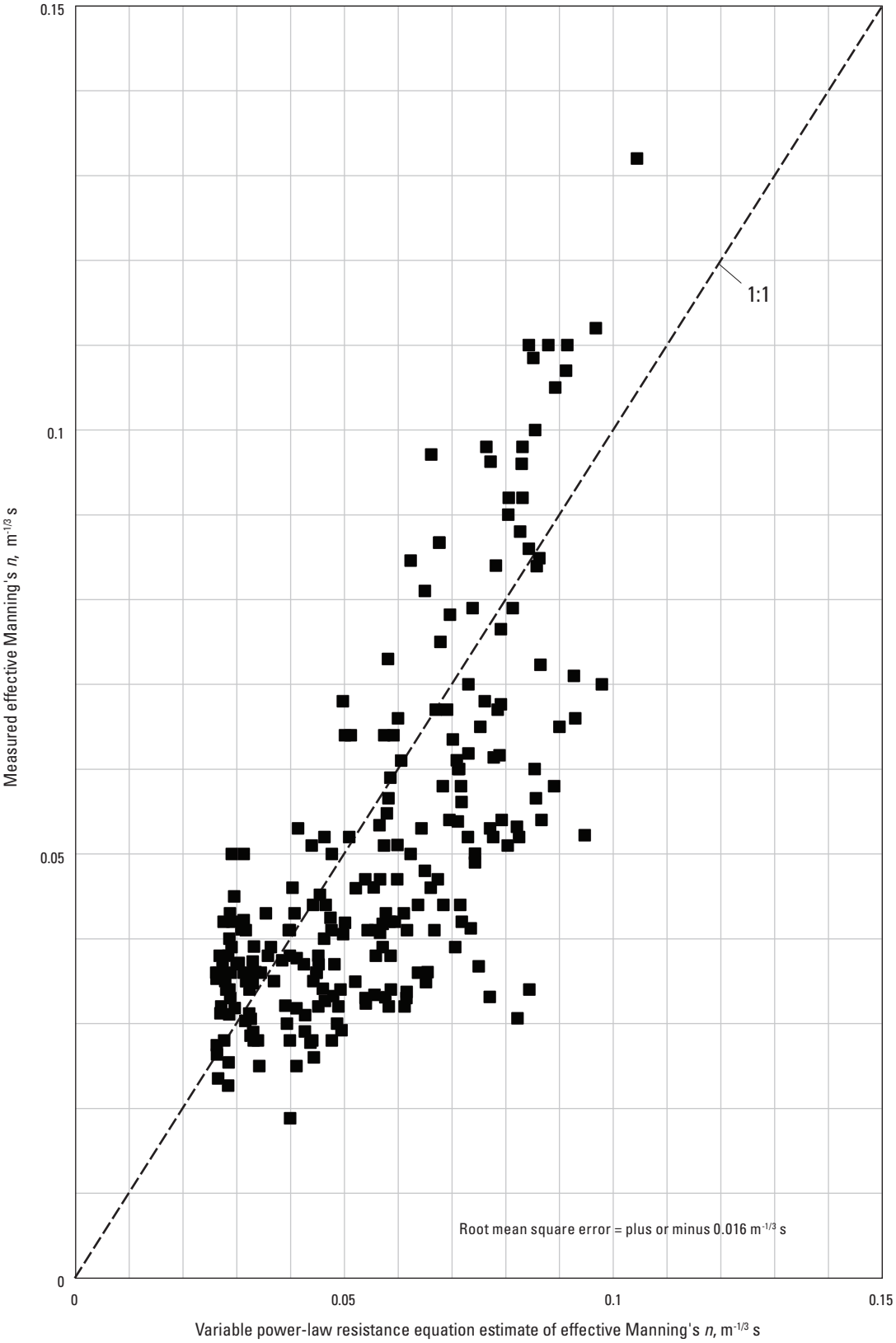

Figure 4. Comparison of measure effective Manning's *n* and variable power law resistance equation estimate of effective Manning's *n*. Parameters values (c_1=7.3 and c_2=2.3) for a variable-power law (Ferguson, 2007) were selected to fit measured values of *n* for sites with similar conditions to the steep, mountainous sites in this report. [$m^{-1/3}$ s, meter to the minus one-third power times second]

Measured "n" Method

The Sugarloaf research site was established on a north-facing hillslope to measure rainfall and runoff after the 2010 Fourmile Canyon wildfire (Ebel and others, 2012). Measurements were made of overland flow velocities in the small basin (0.0084 km^2) composing most of the research site. Water was released from a 20-liter (L) jug at several locations within the small basin at a maximum rate of 0.05 liter per second (L s^{-1}), and velocities were computed from the measured travel time of dye or particles in the water between two points separated by a known distance. The local slopes were measured between the two points, and the depth of flow was estimated to be about 5 mm. Manning's *n* was then calculated using the average slope and average velocity at each location. This set of measurements gave an average value of n =0.21 $m^{-1/3}$ s with standard deviation of 0.07 $m^{-1/3}$ s.

Yochum Method

The Sugarloaf hillslope channel had the steepest average slope (0.37) and most resembled a step-pool type of channel (Yochum and others, 2012) 3 years after the wildfire. This type of channel was created by episodic and not perennial flow, which was characteristic of most other sites. For steep channel slopes (0.015–0.20), the Yochum method is an empirical velocity equation that uses the standard deviation of longitudinal profiles of the channel bed, (σ_z, in meters), as the roughness metric instead of the relative submergence (R/D_{84}); however, other researchers have had varying degrees of success using R/D_{84} (Yochum and others, 2012). Using an estimate of $D_{84} \approx 2\,\sigma_z$ indicates that the R/D_{84} was <1 for the datasets used to develop this empirical equation. The use of σ_z assumes that the characteristic roughness, for step-pool channels investigated by Yochum and others (2012), varies only in the down-channel direction (as indicated by published values of the step-wavelength metric) where spill resistance is typically dominant and cross-channel roughness because of particle or form roughness is not (Yochum and others, 2012; Comiti and others 2007). The nondimensional model 17 listed in Yochum and others (2012, table 6) was selected based on the high value of R^2. The dimensional version is:

$$v = 0.93\left(\frac{h}{\sigma_z}\right)\left(gSh\right)^{1/2} \qquad (6)$$

The value of σ_z was 0.054 m based on a single longitudinal profile with a spacing interval of 0.05 m. This roughness value seemed too small based on field observations and photographs of the Sugarloaf hillslope channel showing a substantial degree of cross-channel roughness. Computed velocities using σ_z =0.054 m were physically unrealistic at some cross sections (>5 m s^{-1}); therefore, the σ_z was set equal to the measured value of D_{84} (0.110 m$\approx 2\,\sigma_z$), which gave more realistic velocities. This relation was applied to each increment of width in the main channel.

Comiti Method

This method developed another empirical velocity equation applicable for steep channel slopes (0.02–0.19) but uses D_{84} instead of σ_z that is used in equation 6. The R/D_{84} was <1 for all datasets used to develop this empirical equation. Converting the nondimensional form (equation 11 and fig. 7 in Comiti and others, 2007) to the dimensional form gives:

$$v = 0.78 g^{\frac{1}{2}} h^{0.50} \left(\frac{h}{D_{84}}\right)^{1.45}, \qquad (7)$$

which is independent of channel slope. This relation was applied to each increment of width in the main channel.

Sediment-Transport Effect

Sediment-transport resistance is not included explicitly in any flow-resistance equation, but any sediment-transport resistance present in the flow is probably accounted for in each resistance equation by using a different value of the coefficient "*a*" for the effective bed-roughness (that is, aD_{84}). For steep, mountain streams where D_{84} >32 mm and for typical flood depths of 1–3 m, the non dimensional Rouse number, $z = w/\kappa u_*$, is generally >1.5 (w is the particle settling velocity, [m s^{-1}], κ is von Kármán constant = 0.41 (Chow, 1964) and $u_* = \sqrt{gRS}$, is the shear velocity [m s^{-1}]. For z >1.5, most particles >32 mm would not move as suspended load but rather as bedload (Ned Andrews, U.S. Geological Survey [ret.], oral commun., 2013), which increases flow resistance (Smith and McLean, 1977; Pitlick, 1992; Campbell and others, 2005; Zhang and others, 2010) by extracting energy from the mean flow (Wang and Larsen, 1994; Pierson, 2005). Sediment transport effects must have been a primary component of the flow resistance during the September 2013 floods given the documentation in the media of numerous eroded roads and highways alongside channels and the extensive areas of sediment deposition affecting private and public infrastructure (fig. 5).

It is understandable why, given the flow conditions encountered during floods, no bedload and ancillary data exist to determine a relation between a flow-resistance parameter (for example, Manning's *n*) and the unit bedload transport rate (q_s in kilograms per meter times seconds [kg m^{-1} s^{-1}]) that could be used to estimate peak flood discharges. Order of magnitude estimates of bedload transport for conditions typical of the September 2013 floods are 10–1,000 kg m^{-1} s^{-1} based on extrapolating the bedload equation developed by Luque and Beek (1976) and used by Yager and others (2007). Most field measurements of q_s are generally less than bankfull and <1 kg m^{-1} s^{-1} (for

Figure 5. Typical examples of erosion and deposition of sediment from the September 2013 floods, Boulder County, Colorado. *A*, View downstream of bank erosion, and road and utility damage caused by the flood waters of James Creek below Jamestown, Colorado. Photograph was taken on September 13, 2013, by Mark Williams. *B*, View downstream of a depositional reach above Jamestown, Colorado, on James Creek and downstream from Moorhead Gulch where there was a landslide/debris flow that probably blocked the old channel (left side) until the water eroded out a new channel (right side). Photograph taken on April 28, 2014.

example, Milhous, 1973; Gomez, 1991; Bunte, 1996; Ryan and Emmett, 2002); however, some flume experiments using smaller particles (≈10 mm) have measured rates up to about 100 kg m^{-1} s^{-1} (Smart, 1984). Zhang and others (2010) found an empirical power-law relation between Manning's *n* and bedload transport rate (<7 kg m^{-1} s^{-1}), and analyzing data published by Smart (1984) gave a similar relation:

$$n = 0.026 q_s^{0.176}; R^2 = 0.44 \quad (8)$$

for near-uniform particle size of D_{50}=10.4 mm and q_s<75 kg m^{-1} s^{-1}. This equation gives a reasonable range of *n* from 0.039 to 0.087 $m^{-1/3}$ s corresponding to the possible range of q_s from 10 to 1,000 kg m^{-1} s^{-1}. Similar relations, with lower values of R^2, were determined for smaller D_{50} (4.2 mm) and for nonuniform particle sizes (D_{50}=2.0 and 4.3 mm).

Equation 8 was applied to each width increment in the main channel to give an extrapolated estimate of *n* and, thus, a separate sediment-transport-based estimate of the peak discharge. Values of *n* determined by the Cowan method were used for the adjacent flood plains. This estimate of peak discharge based on sediment-transport effects was not included in the ensemble average because it is based on smaller particle sizes than were typical for the September 2013 floods and required an extrapolation beyond the conditions on which it is based; however, it provides an estimate of the potential effect of bedload transport on peak discharges and, thus, a comparison for the other methods.

Rainfall Intensity Calculations

Cumulative rainfall data during the September 2013 storms were available from the Urban Drainage and Flood Control District (http://udfcd.org/), which maintains more than 36 tipping-bucket recording rain gages in Boulder County, Colo. If a hydrograph is available, then the "volume runoff-coefficient" can be calculated as the total volume of discharge for a specified time interval divided by the total volume of accumulated rainfall for the same time interval; however, for the September 2013 floods, most streamgages were damaged and did not record a full hydrograph, or the stream was ungaged. For these sites, the runoff coefficient was estimated using what is referred to in this report as the "peak runoff-coefficient" where the unit peak discharge (Q_u, in cubic meters per second per square kilometer [m^3 s^{-1} km^{-2}]; peak discharge divided by the drainage area), is divided by the average peak rainfall intensity of the upstream rain gages that were within or on the boundary of the drainage area for the measurement site. As a first approximation, a simple average was used for most sites because the density of rain gages was relatively uniform. It is important to remember that the "peak runoff-coefficient" tends to overestimate the runoff coefficient because any number of hydrograph shapes could have the same peak discharge but different volume runoff coefficients. The use of the "peak runoff-coefficient" is intended to provide relative comparisons between basins and a first-order check (that is, conservation of mass) on the value of the peak discharge.

The appropriate time interval for computing the peak rainfall intensity depends on the drainage area upstream from the indirect measurement site and was based on the physical property of a basin referred to as the time-to-concentration (T_c, in minutes [min]). This is the "time required for runoff to travel from the hydraulically most distant point in the watershed to the outlet. The hydraulically most distant point is the point with the longest travel time to the watershed outlet, and not necessarily the point with the longest flow distance to the outlet" (Natural Resources Conservation Service, 2010, p. 15–3). The empirical equation is:

$$T_c = \frac{L^{0.8}\left(M+1\right)^{0.7}}{1140 Y^{0.5}} \quad (9)$$

where

L is the longest path, in meters
M is the maximum potential retention, in meters and
Y is the average watershed slope, in prcent.

Values for *L* and *Y* for each site were determined from a 30-m digital elevation model (DEM) using the River Tools software (RIVIX, LLC; www.rivertools.com) specialized for analyzing the topographic characteristics of river basins. The maximum potential retention (*M*) is extremely difficult to estimate with any certainty for mountainous areas, which had already had 50–100 mm of rain by the evening of September 11, 2013. As a first approximation, *M* can be assumed to be 0 given the nearly saturated conditions that existed on the evening of September 11 before the time of the peak discharges in the early morning hours of September 12, 2013. A value of *M*=0 is equivalent to a curve number of 100 (see Woodward and others [2003] for discussion of the curve number method). Values of T_c were computed for each measurement site (table 1) and rounded to the nearest 10-min, one-half or 1-h interval (except Sugarloaf was 2 min) to determine the average peak rainfall intensity.

These rain gage records are time series but have an irregular time interval corresponding to the time between each tip equal to 1.0 mm. Cumulative rainfall was interpolated and redigitized to produce a time series with a regular interval of 2 minutes, and peak rainfall intensities were computed as a central difference using the rounded value of T_c.

Estimates of Peak Discharge

The estimates of peak discharge are organized by basins from the northern to the southern part of Boulder County. The brief descriptions below for each measurement site highlight any special features or condition which augments the summary in table 1 and photographs that characterizes the channel at each measurement site.

North St. Vrain Creek above Highway 7 Bridge

The indirect peak discharge (18 $m^3 s^{-1}$, tables 1 and 2) was measured on November 1, 2014, and the surveyed reach (fig. 6) started 50 m upstream from the discontinued gage site (North Saint (St.) Vrain Creek near Allens Park operated by Colorado Division of Water Resources). North St. Vrain Creek (fig. 1*B* and 1*C*) drains an alpine area above 2,500 m that was on the edge of the high-accumulation, high-intensity region (fig. 1*C*). No rain gages were located within this alpine area or near its boundaries; therefore, based on the rainfall pattern shown in figure 1*C*, the average peak rainfall intensity of (6.8 millimeters per hour [mm h^{-1}]for the Hills Mills rain gage (at about the same elevation as the alpine area) was used (table 1). Peak discharge at this site was in response to the lowest average rainfall intensity at any site and had one of the lowest bed slopes (0.011, table 1). The different indirect methods estimated that 82–97 percent of the flow was in the main channel (fig. 6).

Figure 6. North Saint Vrain Creek above Highway 7 Bridge. *A*, Upstream view taken at 0917 on September 12, 2013 by Glenn Patterson. *B*, Upstream view taken on November 1, 2014. The distance from the bottom of the white sign to the streambed was 0.5 meters.

Table 2. Summary of indirect discharge measurements for North St. Vrain Creek above Highway 7 Bridge, Boulder County, Colorado.

[ID, cross section identification; XS, cross section; LB, left bank; RB, right bank; HW, high-water mark; SAC, slope-area calculation; stdev, standard deviation; COV, coefficient of variation; m, meter; m^2, square meter; ms^{-1}, meter per second; $m^3 s^{-1}$, cubic meter per second; na, not applicable]

ID	Distance from arbitrary zero (m)	Arbitrary elevation			Hydraulic radius (m)	Depth (m)	Width (m)	Area (m^2)	Mean cross-sectional velocity				Discharge					
		LB HW (m)	RB HW (m)	Thalweg (m)					Jarrett ($m\ s^{-1}$)	Cowan ($m\ s^{-1}$)	Empirical ($m\ s^{-1}$)	Critical flow ($m\ s^{-1}$)	Jarrett ($m^3\ s^{-1}$)	Cowan ($m^3\ s^{-1}$)	Empirical ($m^3\ s^{-1}$)	Critical flow ($m^3\ s^{-1}$)	SAC[1] ($m^3\ s^{-1}$)	Ensemble average ($m^3\ s^{-1}$)
XS1	61.7	100.31	100.25	99.02	0.8	0.8	14.3	11.3	0.2	2.5	2.5	2.9	19	29	29	33	--	na
XS2	54.1	100.22	100.20	99.03	0.7	0.8	15.9	12.1	1.6	2.2	2.4	2.8	19	29	29	34	--	na
XS3	44.4	99.96	100.07	99.10	0.6	0.6	16.6	10.1	1.3	2.0	1.9	2.5	13	21	19	25	21	na
XS4	38.1	99.87	99.87	98.94	0.5	0.6	13.5	7.5	1.2	2.0	1.7	2.5	9	15	13	18	15	na
XS5	25.9	na	99.76	98.77	0.5	0.6	13.7	7.7	1.2	1.9	1.7	2.3	9	14	13	18	15	na
XS6	12.9	99.71	99.85	98.78	0.7	0.7	12.0	8.8	1.3	1.9	1.7	2.2	11	16	15	19	12	na
XS7	0.0	99.39	99.60	98.27	0.8	0.8	9.0	7.5	1.7	2.5	2.5	2.9	12	19	18	22	--	na
												Average	13	20	19	24	[2]15	18
												stdev	4.3	6.1	6.8	6.9	3.7	4.4
												COV	0.32	0.30	0.35	0.29	na	0.26

[1]Spread is the percent difference between discharge computed with no expansion loss and discharge computed with full expansion loss, divided by the discharge computed with full expansion loss. Cross sections with spreads >1 are shown by --.

[2]This is the average energy balanced value for the reach given above that had the minimum spread of 0–1 percent.

North St. Vrain Creek above Apple Valley Bridge

The indirect peak discharge (385 $m^3 s^{-1}$, tables 1 and 3) was measured on March 9, 2014, after some of the left-bank, high-water marks had been destroyed by blasting at the mouth of North St. Vrain Canyon for flood repair work on U.S. Highway 36 (fig. 7). Manning's *n* was selected for four subareas (highway, left bank, main channel, and right bank) of each cross section. Flow at this measurement site was modified by flow from the Button Rock Reservoir located about 5.7 km upstream from this site. Bed slope was the lowest of all sites (0.006, table 1). The different indirect methods estimated that 91–94 percent of the flow was in the main channel (fig. 7).

Figure 7. North Saint Vrain Creek above Apple Valley Bridge on November 12, 2013. View is upstream from the Apple Valley Bridge. Flood waters had covered Highway 36 (on the right-hand side of the photo) to a depth of 0.3–0.5 meter.

Table 3. Summary of indirect discharge measurements for North St. Vrain Creek above Apple Valley Bridge, Boulder County, Colorado.

[ID, cross section identification; XS, cross section; LB, left bank; RB, right bank; HW, high-water mark; SAC, slope-area calculation; stdev, standard deviation; COV, coefficient of variation; m, meter; m^2, square meter; ms^{-1}, meter per second; $m^3\ s^{-1}$, cubic meter per second; na, not applicable]

ID	Distance from arbitrary zero (m)	Arbitrary elevation			Hydraulic radius (m)	Depth (m)	Width (m)	Area (m^2)	Mean cross-sectional velocity				Discharge					
		LB HW (m)	RB HW (m)	Thalweg (m)					Jarrett ($m\ s^{-1}$)	Cowan ($m\ s^{-1}$)	Empirical ($m\ s^{-1}$)	Critical flow ($m\ s^{-1}$)	Jarrett ($m^3\ s^{-1}$)	Cowan ($m^3\ s^{-1}$)	Empirical ($m^3\ s^{-1}$)	Critical flow ($m^3\ s^{-1}$)	SAC[1] ($m^3\ s^{-1}$)	Ensemble average ($m^3\ s^{-1}$)
XS1	198	99.31	99.49	95.47	1.9	2.0	47.9	95.0	4.4	5.4	6.7	5.1	422	512	636	487	--	na
XS2	167.5	98.82	98.98	95.08	1.8	1.9	44.6	83.2	3.8	4.5	5.6	4.4	320	377	469	363	--	na
XS3	137.0	98.77	98.90	94.90	2.1	2.1	44.8	95.7	4.2	5.0	6.1	4.7	404	476	585	453	--	na
XS4	106.5	98.50	98.79	94.54	2.0	2.2	42.8	94.9	4.4	5.2	6.4	5.0	418	497	607	475	254	na
XS5	76	98.00	97.78	94.47	1.7	2.0	39.7	77.9	3.8	4.7	5.7	4.6	296	366	446	355	507	na
XS6	46	97.71	98.39	94.25	2.0	2.1	38.1	81.8	4.6	5.5	6.7	5.3	376	448	544	432	260	na
XS7	15	97.50	97.05	94.32	1.6	1.7	35.8	61.3	3.5	4.4	5.4	4.4	217	271	330	269	231	na
XS8	0	97.28	97.28	94.42	1.7	1.8	37.8	68.6	3.7	4.5	5.5	4.5	251	312	380	309	--	na
												Average	338	407	500	393	[2]288	385
												stdev	79	89	111	80	130	80
												COV	0.23	0.22	0.22	0.20	na	0.21

[1]Spread is the percent difference between discharge computed with no expansion loss and discharge computed with full expansion loss, divided by the discharge computed with full expansion loss. Cross sections with spreads >1 are shown by --.

[2]This is the average energy balanced value for the reach given above that had the minimum spread of 0–1 percent.

South St. Vrain Creek above Confluence with Middle St. Vrain Creek

The indirect peak discharge (66 $m^3 s^{-1}$, tables 1 and 4) was measured on May 16, 2014, and was one of the few sites not located alongside a county road or State or Federal highway. Water is diverted during the irrigation season from South St. Vrain Creek into James Creek near the headwaters of the South St. Vrain Creek. This diversion was in operation during the peak flow on the night of September 11–12, 2013, so the drainage areas of the South St. Vrain and James Creeks have been adjusted to reflect this diversion (see footnote in table 1). The different indirect methods estimated that 96–98 percent of the flow was in the main channel (fig. 8).

Figure 8. South Saint Vrain Creek above confluence with Middle Saint Vrain Creek on May 16, 2014. View is upstream from cross section 2 (XS2, table 4). Water is diverted from this creek into James Creek for irrigation; thus, the channel conveys less water than its size would suggest. The survey level is about 1.5 meters above the streambed.

Table 4. Summary of indirect discharge measurements for South St. Vrain above confluence with Middle St. Vrain Creek, Boulder County, Colorado.

[ID, cross section identification; XS, cross section; LB, left bank; RB, right bank; HW, high-water mark; SAC, slope-area calculation; stdev, standard deviation; COV, coefficient of variation; m, meter; m^2, square meter; ms^{-1}, meter per second; $m^3 s^{-1}$, cubic meter per second; na, not applicable]

ID	Distance from arbitrary zero (m)	Arbitrary elevation			Hydraulic radius (m)	Depth (m)	Width (m)	Area (m^2)	Mean cross-sectional velocity				Discharge					
		LB HW (m)	RB HW (m)	Thalweg (m)					Jarrett ($m\ s^{-1}$)	Cowan ($m\ s^{-1}$)	Empirical ($m\ s^{-1}$)	Critical flow ($m\ s^{-1}$)	Jarrett ($m^3\ s^{-1}$)	Cowan ($m^3\ s^{-1}$)	Empirical ($m^3\ s^{-1}$)	Critical flow ($m^3\ s^{-1}$)	SAC[1] ($m^3\ s^{-1}$)	Ensemble average ($m^3\ s^{-1}$)
XS1	105	102.25	102.18	100.24	1.0	1.2	14.1	17.0	2.4	4.0	5.0	3.3	41	68	84	56	--	na
XS2	90	na	101.82	99.89	1.2	1.3	16.0	21.5	2.7	4.4	5.5	3.6	59	95	117	78	--	na
XS3	75	101.19	na	99.14	1.1	1.2	14.9	17.8	2.6	4.2	5.2	3.5	46	75	92	62	60	na
XS4	58	100.39	100.43	98.69	1.1	1.2	13.4	16.2	2.5	4.0	4.9	3.3	40	65	80	54	75	na
XS5	45	100.00	99.91	97.92	0.9	0.9	16.8	15.4	2.4	4.0	4.8	3.3	36	61	74	51	79	na
XS6	30	99.86	99.73	97.46	1.1	1.2	16.6	19.7	2.8	4.3	5.6	3.4	55	84	109	67	59	na
XS7	15	99.35	99.10	97.39	1.0	1.2	14.1	16.4	2.3	3.6	4.5	3.0	38	59	73	50	62	na
XS8	0	99.01	99.09	96.97	1.1	1.1	16.2	17.6	2.8	4.4	5.6	3.5	49	76	99	61	50	na
												Average	46	73	91	60	[2]62	66
												stdev	8.1	12.1	16.4	9.5	11.0	17
												COV	0.18	0.17	0.18	0.16	na	0.26

[1]Spread is the percent difference between discharge computed with no expansion loss and discharge computed with full expansion loss, divided by the discharge computed with full expansion loss. Cross sections with spreads >1 are shown by --.

[2]This is the average energy balanced value for the reach given above that had the minimum spread of 0–1 percent.

South St. Vrain Creek below Confluence with Middle St. Vrain Creek

The indirect peak discharge (123 $m^3 s^{-1}$, tables 1 and 5) was measured on March 26, 2014. Much of the South St. Vrain channel was modified after the 2013 flood during repairs to Highway 7 and for flood remediation. The reach for this measurement site was not adjacent to the Highway 7 and was protected from such activity because it had a small intervening flood plain. Although the mass of water must be conserved, the sum of peak discharges above a confluence does not necessarily equal the peak discharge below a confluence because peak discharge at the confluence is not necessarily simultaneous, and peak values may be attenuated with distance downstream (Gilcrest, 1950). For example, the sum of the peak discharge for the North St. Vrain Creek above Apple Valley Bridge (385 $m^3 s^{-1}$) and this site (123 $m^3 s^{-1}$) is 508 $m^3 s^{-1}$. This sum is less than the value (675 $m^3 s^{-1} \pm 10$ percent) estimated downstream from the confluence of the North St. Vrain and South St. Vrain Creeks in Lyons, Colo. (fig. 1*B*) by the U.S. Geological Survey's Colorado Water Science Center using a two-dimensional hydraulic model (http://nwis.waterdata.usgs.gov/co/nwis/peak/?site_no=06724000&agency_cd=USGS; R. Kimbrough, U.S. Geological Survey, written commun., 2015). This estimated combined flow downstream from the confluence was not confined to a single channel but spread out over a wide flood plain with many channels and damaged and destroyed many homes (Lukas, 2013). The different indirect methods estimated that 95–97 percent of the flow was in the main channel (fig. 9).

Figure 9. South Saint Vrain Creek below confluence with Middle Saint Vrain Creek on March 26, 2014. View is upstream from cross section 5 (XS5, table 5). Highway 7 (upper right) is running next to the narrow flood plain along the left bank.

Table 5. Summary of indirect discharge measurements for South St. Vrain below confluence with Middle St. Vrain Creek, Boulder County, Colorado.

[Highlighted cells represent the quality of the high-water mark. ID, cross section identification; XS, cross section; LB, left bank; RB, right bank; HW, high-water mark; SAC, slope-area calculation; stdev, standard deviation; COV, coefficient of variation; m, meter; m^2, square meter; ms^{-1}, meter per second; $m^3\ s^{-1}$, cubic meter per second; na, not applicable]

ID	Distance from arbitrary zero (m)	Arbitrary elevation			Hydraulic radius (m)	Depth (m)	Width (m)	Area (m^2)	Mean cross-sectional velocity				Discharge					
		LB HW (m)	RB HW (m)	Thalweg (m)					Jarrett ($m\ s^{-1}$)	Cowan ($m\ s^{-1}$)	Empirical ($m\ s^{-1}$)	Critical flow ($m\ s^{-1}$)	Jarrett ($m^3\ s^{-1}$)	Cowan ($m^3\ s^{-1}$)	Empirical ($m^3\ s^{-1}$)	Critical flow ($m^3\ s^{-1}$)	SAC[1] ($m^3\ s^{-1}$)	Ensemble average ($m^3\ s^{-1}$)
XS1	132	101.02	101.19	98.61	1.3	1.4	21.2	30.6	2.9	3.9	4.8	4.0	90	119	147	121	--	na
XS2	113	101.01	100.90	98.22	1.6	1.7	20.2	34.3	2.6	3.2	4.0	3.2	88	110	139	108	--	na
XS3	89	100.66	100.37	97.77	1.6	1.7	22.6	37.5	3.1	4.0	5.1	3.9	117	149	190	147	--	na
XS4	71	99.79	100.07	97.48	1.4	1.5	22.6	33.1	2.7	3.4	4.3	3.4	90	113	144	112	102	na
XS5	51	99.46	99.28	96.81	1.3	1.4	18.5	26.4	2.9	3.8	4.7	3.8	76	100	123	102	112	na
XS6	31	98.99	99.45	96.49	1.4	1.5	24.5	35.9	2.9	3.6	4.6	3.6	103	130	165	129	67	na
XS7	14	99.05	99.20	96.16	1.6	1.6	25.8	41.8	3.1	3.8	5.0	3.7	129	160	207	156	--	na
XS8	0	98.48	98.70	95.81	1.5	1.6	24.8	40.3	3.0	3.8	4.8	3.7	121	152	195	150	--	na
		Good										**Average**	102	129	164	128	[2]94	123
		Fair										**stdev**	18.9	22.1	30.4	20.6	23.3	27
		Poor										**COV**	0.19	0.17	0.19	0.16	na	0.22
		Very poor																

[1]Spread is the percent difference between discharge computed with no expansion loss and discharge computed with full expansion loss, divided by the discharge computed with full expansion loss. Cross sections with spreads >1 are shown by --.

[2]This is the average energy balanced value for the reach given above that had the minimum spread of 0–1 percent.

Little James Creek above Confluence with James Creek

The indirect peak discharge (74 $m^3 s^{-1}$, tables 1 and 6) was measured on March 19, 2014, in a reach with a channel bed composed of mostly bedrock outcrops, which complicated the measurement of D_{84}. It seems that the Manning's n value based on the Cowan method (0.15 $m^{-1/3}$ s along the banks and 0.043 $m^{-1/3}$ s in the main channel) and the Empirical methods may be too low because the mean cross-sectional velocities for the Cowan method (table 6) were generally >5.3 m s^{-1}, whereas the mean cross-sectional velocities for the Jarrett and Critical Flow methods were around 3 m s^{-1}; however, deleting the Cowan and Empirical methods would only reduce the ensemble average from 74 to 61 $m^3 s^{-1}$ and change the peak runoff coefficient from 1.4 to 1.2. A separate indirect discharge measurement for the same reach used only the Critical flow method and reported 51 $m^3 s^{-1}$ (Yochum and Moore, 2013), which is essentially the same as the average value for the Critical flow method in table 6 (54 $m^3 s^{-1}$). The drainage area (7.76 km^2) is small, but the unit peak discharge (9.5 $m^3 s^{-1} km^{-2}$, table 1) is large, which may be the result of increased runoff from part of the area burned by the 2003 Overland fire (Kinner and Moody, 2008). Several landslide/debris flows were generated during the evening of September 11–12, 2013, on Porphyry Mountain within the drainage basin of Little James Creek. Only one rain gage (Porphyry Mountain, fig. 1*C*) was used to calculate the peak rainfall intensity for T_c about=1 h, and this may underestimate the rainfall intensity. The 30- and 10-min peak rainfall intensities were 29.4 and 44.3 mm h^{-1} corresponding to peak runoff coefficients of 1.0 and 0.77, respectively. Runoff coefficients this large suggest that the T_c might be much shorter than estimated, but the possible reasons are not apparent. The different indirect methods estimated that 72–90 percent of the flow was in the main channel (fig. 10).

Figure 10. Little James Creek above confluence with James Creek on March 19, 2014. View is upstream from cross section 1 (XS1, table 6). The steel tagline is about 0.1–0.2 meter above the high-water elevation. The channel is about 5 meters wide below the steel tagline.

Table 6. Summary of indirect discharge measurements for Little James Creek above confluence with James Creek, Boulder County, Colorado.

[Highlighted cells represent the quality of the high-water mark. ID, cross section identification; XS, cross section; LB, left bank; RB, right bank; HW, high-water mark; SAC, slope-area calculation; stdev, standard deviation; COV, coefficient of variation; m, meter; m^2, square meter; ms^{-1}, meter per second; $m^3\ s^{-1}$, cubic meter per second; na, not applicable]

ID	Distance from arbitrary zero (m)	Arbitrary elevation			Hydraulic radius (m)	Depth (m)	Width (m)	Area (m^2)	Mean cross-sectional velocity				Discharge					
		LB HW (m)	RB HW (m)	Thalweg (m)					Jarrett ($m\ s^{-1}$)	Cowan ($m\ s^{-1}$)	Empirical ($m\ s^{-1}$)	Critical flow ($m\ s^{-1}$)	Jarrett ($m^3\ s^{-1}$)	Cowan ($m^3\ s^{-1}$)	Empirical ($m^3\ s^{-1}$)	Critical flow ($m^3\ s^{-1}$)	SAC[1] ($m^3\ s^{-1}$)	Ensemble average ($m^3\ s^{-1}$)
XS1	0	99.69	100.04	97.87	0.7	0.8	20.0	16.2	3.3	5.4	6.2	3.9	53	87	100	62	--	na
XS2	16	100.71	100.55	98.30	1.1	1.1	14.4	16.5	2.7	5.4	6.6	3.3	44	89	109	54	--	na
XS3	30	101.11	101.38	99.10	1.1	1.2	12.4	15.3	5.9	5.8	7.1	3.5	90	88	108	53	--	na
XS4	44	101.89	102.21	99.76	1.2	1.3	13.9	17.5	2.8	5.3	6.5	3.3	49	93	115	57	69	na
XS5	57	102.35	102.69	100.31	1.2	1.3	13.1	17.5	2.9	5.3	6.5	3.3	50	93	114	57	98	na
XS6	71	102.79	102.80	100.75	1.1	1.2	11.5	14.0	2.8	5.5	6.7	3.3	39	76	94	47	68	na
XS7	93	103.79	104.21	101.78	1.1	1.3	11.7	14.9	2.7	4.9	5.9	3.1	40	72	88	46	--	na
		Good										**Average**	52	86	104	54	[2]76	74
		Fair										**stdev**	17.5	8.1	10.2	6.0	16.7	22
		Poor										**COV**	0.34	0.10	0.10	0.11	na	0.30
		Very poor																

[1]Spread is the percent difference between discharge computed with no expansion loss and discharge computed with full expansion loss, divided by the discharge computed with full expansion loss. Cross sections with spreads >1 are shown by --.

[2]This is the average energy balanced value for the reach given above that had the minimum spread of 0–1 percent.

James Creek above Jamestown

The indirect peak discharge (102 $m^3 s^{-1}$, tables 1 and 7) was not measured until October 11, 2014, because of road repair work during the fall of 2013, ice cover during the winter of 2013–14, high flow from snowmelt runoff during the spring of 2014, and the diversion of irrigation water from the South St. Vrain Creek into James Creek during the summer of 2014. Bed roughness on this stream was one of the largest with D_{84} for the vertical or z-axis being 400 mm, the cross-stream axis being 800 mm, and the width/depth ratio being 8.1 (table 1). This channel most resembled Clear Creek near Golden in Barnes (1967); thus, Manning's *n* values for the Cowan method were 0.050 $m^{-1/3}$ s for the main channel and 0.28 $m^{-1/3}$ s for the flood plain (fig. 11). Values estimated by the Empirical method ranged from 0.037 to 0.071 $m^{-1/3}$ s. Both sets of *n* seem low because the mean cross-sectional velocities in the main channel ranged from 6.3 to 9.9 m s^{-1}, and the average peak discharge of the six cross sections (133 $m^3 s^{-1}$, Cowan method and 158 $m^3 s^{-1}$, Empirical method; table 7) was about twice the estimates using the other methods except for the SAC method estimate (86 $m^3 s^{-1}$). The different indirect methods estimated that 95–98 percent of the flow was in the main channel (fig. 11).

Figure 11. James Creek above Jamestown, Colorado, on October 11, 2014. View is downstream from right bank at cross section 1 (XS1, table 7). Photograph taken by G. Patterson.

Table 7. Summary of indirect discharge measurements for James Creek above Jamestown, Boulder County, Colorado.

[Highlighted cells represent the quality of the high-water mark. ID, cross section identification; XS, cross section; LB, left bank; RB, right bank; HW, high-water mark; SAC, slope-area calculation; stdev, standard deviation; COV, coefficient of variation; m, meter; m^2, square meter; ms^{-1}, meter per second; $m^3\ s^{-1}$, cubic meter per second; na, not applicable]

ID	Distance from arbitrary zero (m)	Arbitrary elevation			Hydraulic radius (m)	Depth (m)	Width (m)	Area (m^2)	Mean cross-sectional velocity				Discharge					
		LB HW (m)	RB HW (m)	Thalweg (m)					Jarrett ($m\ s^{-1}$)	Cowan ($m\ s^{-1}$)	Empirical ($m\ s^{-1}$)	Critical flow ($m\ s^{-1}$)	Jarrett ($m^3\ s^{-1}$)	Cowan ($m^3\ s^{-1}$)	Empirical ($m^3\ s^{-1}$)	Critical flow ($m^3\ s^{-1}$)	SAC[1] ($m^3\ s^{-1}$)	Ensemble average ($m^3\ s^{-1}$)
XS1	41	102.75	102.75	100.04	1.5	1.7	14.3	24.9	4.0	8.2	8.7	4.3	99	204	217	106	--	na
XS2	31	101.80	101.57	98.96	1.0	1.7	10.3	17.5	3.5	7.4	9.4	3.9	62	128	164	67	--	na
XS3	25	101.48	na	98.87	1.4	1.7	10.6	18.4	3.7	7.8	9.9	4.1	68	144	182	76	--	na
XS4	16	100.45	100.91	98.47	1.3	1.5	10.7	16.0	3.2	6.8	8.5	3.7	52	109	135	59	83	na
XS5	9	100.15	na	98.19	1.0	1.2	12.6	15.1	3.0	6.7	7.9	3.7	46	101	119	56	122	na
XS6	0	99.88	99.82	97.77	1.1	1.2	12.9	16.1	2.9	6.3	7.4	3.5	46	101	119	56	60	na
		Good										**Average**	63	133	158	72	[2]86	102
		Fair										**stdev**	20.2	39.7	38.9	19.4	31.1	41
		Poor										**COV**	0.32	0.30	0.25	0.27	na	0.40
		Very poor																

[1]Spread is the percent difference between discharge computed with no expansion loss and discharge computed with full expansion loss, divided by the discharge computed with full expansion loss. Cross sections with spreads >1 are shown by --.

[2]This is the average energy balanced value for the reach given above that had the minimum spread of 0–1 percent.

James Creek below Jamestown

The indirect peak discharge (122 m^3/s, tables 1 and 8) was measured on April 23, 2014, after the ice had melted. This measurement site was below the confluence of Little James Creek (74 $m^3 s^{-1}$) and James Creek above Jamestown (102 $m^3 s^{-1}$), and one reason why the sum of the upstream discharges (176 $m^3 s^{-1}$) does not equal the downstream discharge at this site might be because the peak discharges on Little James and James Creeks at the confluence were not simultaneous. Mark Williams, a resident of Jamestown, observed that James Creek had several surges probably in response to landslide/debris flows temporarily blocking the stream and then eroding out. One such landslide/debris flow from Moorhead Gulch blocked James Creek about 450 m downstream from the James Creek above Jamestown site, and about 750 m upstream from the confluence of Little James and James Creek. Another reason for the difference is the attenuation of the peak discharge with distance downstream (Gilcrest, 1950). A separate estimate made in Jamestown was 136 $m^3 s^{-1}$ (Yochum and Moore, 2013), which is closer to the sum of Little James Creek and James Creek above Jamestown. The different indirect methods estimated that 90–95 percent of the flow was in the main channel (fig. 12).

Figure 12. James Creek below Jamestown, Colorado, on November 20, 2013. View is upstream from right bank at cross section 5 (XS5, table 8). Cross section 1 is about where the creek disappears behind the left-bank flood plain. Highway 7 (top right) is at the top of the bare bank.

Table 8. Summary of indirect discharge measurements for James Creek below Jamestown, Boulder County, Colorado.

[Highlighted cells represent the quality of the high-water mark. ID, cross section identification; XS, cross section; LB, left bank; RB, right bank; HW, high-water mark; SAC, slope-area calculation; stdev, standard deviation; COV, coefficient of variation; m, meter; m^2, square meter; ms^{-1}, meter per second; $m^3\ s^{-1}$, cubic meter per second; na, not applicable]

ID	Distance from arbitrary zero (m)	Arbitrary elevation			Hydraulic radius (m)	Depth (m)	Width (m)	Area (m^2)	Mean cross-sectional velocity				Discharge					
		LB HW (m)	RB HW (m)	Thalweg (m)					Jarrett ($m\ s^{-1}$)	Cowan ($m\ s^{-1}$)	Empirical ($m\ s^{-1}$)	Critical flow ($m\ s^{-1}$)	Jarrett ($m^3\ s^{-1}$)	Cowan ($m^3\ s^{-1}$)	Empirical ($m^3\ s^{-1}$)	Critical flow ($m^3\ s^{-1}$)	SAC[1] ($m^3\ s^{-1}$)	Ensemble average ($m^3\ s^{-1}$)
XS1	197	102.22	102.37	99.85	1.6	1.7	25.1	42.0	3.7	5.7	7.3	4.3	156	238	304	180	--	na
XS2	167	100.77	101.45	98.36	1.4	1.5	18.0	26.4	3.1	5.2	6.7	3.8	83	136	176	100	--	na
XS3	139	98.98	98.81	96.34	1.4	1.5	23.1	33.8	3.5	5.6	7.1	4.1	117	188	242	139	--	na
XS4	114	97.98	98.00	95.80	1.2	1.2	22.4	27.7	2.8	4.5	5.7	3.4	77	125	158	94	97	na
XS5	83	96.52	97.09	95.20	1.3	1.4	15.9	22.0	3.0	5.0	6.2	3.8	67	110	137	84	88	na
XS6	54	96.25	96.05	93.69	1.4	1.5	14.4	21.5	3.1	5.1	6.7	3.7	67	110	143	80	71	na
XS7	34	95.81	96.01	93.45	1.3	1.4	13.3	19.0	3.1	5.2	6.8	3.8	59	99	129	72	63	na
XS8	0	95.44	94.75	92.59	1.6	1.8	14.3	25.5	3.8	5.9	7.6	4.4	96	150	193	112	89	na
		Good										**Average**	90	144	185	107	[2]83	122
		Fair										**stdev**	32.4	47.2	60.3	36.0	14.1	43
		Poor										**COV**	0.36	0.33	0.33	0.34	na	0.35
		Very poor																

[1]Spread is the percent difference between discharge computed with no expansion loss and discharge computed with full expansion loss, divided by the discharge computed with full expansion loss. Cross sections with spreads >1 are shown by --.

[2]This is the average energy balanced value for the reach given above that had the minimum spread of 0–1 percent.

Left Hand Creek below Nugget Gulch

The indirect peak discharge (52 $m^3 s^{-1}$, tables 1 and 9) was measured on April 9, 2014, above the confluence with James Creek. This was a rough reach (fig. 13) but had a more distinct flood plain than at other sites. The right-bank flood plain was wider than the left-bank flood plain and had numerous small trees (0.10-m diameter) and boulders among the trees (fig. 13) so that the Manning's n was estimated to be 0.25 $m^{-1/3}$ s on the right bank and 0.05 $m^{-1/3}$ s on the left bank with scattered large ponderosa trees (0.30-m diameter) and grass in the intervening spaces. The main channel was rough with the vertical height above the bed or z-axis of D_{84} equal to 380 mm and the cross-stream axis of D_{84} equal to 640 mm (fig. 13). These large boulders occupied 15–50 percent of the cross section, and this channel most resembled Cache Creek near Lower Lake, California, where Manning's n=0.079 $m^{-1/3}$ s (Barnes, 1967). The different indirect methods estimated that 80–88 percent of the flow was conveyed in the main channel (fig. 13), and the remainder was conveyed through the adjacent flood plains.

Figure 13. Left Hand Creek below Nugget Gulch on November 20, 2013. View is upstream from cross section 6 (XS6, table 9).

Table 9. Summary of indirect discharge measurements for Left Hand Creek below Nugget Gulch, Boulder County, Colorado.

[ID, cross section identification; XS, cross section; LB, left bank; RB, right bank; HW, high-water mark; SAC, slope-area calculation; stdev, standard deviation; COV, coefficient of variation; m, meter; m^2, square meter; ms^{-1}, meter per second; $m^3 s^{-1}$, cubic meter per second; na, not applicable]

ID	Distance from arbitrary zero (m)	Arbitrary elevation			Hydraulic radius (m)	Depth (m)	Width (m)	Area (m^2)	Mean cross-sectional velocity				Discharge					
		LB HW (m)	RB HW (m)	Thalweg (m)					Jarrett ($m\ s^{-1}$)	Cowan ($m\ s^{-1}$)	Empirical ($m\ s^{-1}$)	Critical flow ($m\ s^{-1}$)	Jarrett ($m^3\ s^{-1}$)	Cowan ($m^3\ s^{-1}$)	Empirical ($m^3\ s^{-1}$)	Critical flow ($m^3\ s^{-1}$)	SAC[1] ($m^3\ s^{-1}$)	Ensemble average ($m^3\ s^{-1}$)
XS1	120	101.57	101.44	99.64	1.1	1.3	11.0	13.9	3.2	3.7	5.4	3.9	44	52	75	54	--	na
XS2	100	99.60	99.94	98.34	0.9	0.9	10.0	9.2	2.5	2.9	3.9	3.1	23	27	36	29	--	na
XS3	85	99.97	99.65	97.38	1.3	1.5	11.6	17.1	3.3	3.8	6.0	3.7	57	65	102	64	49	na
XS4	69	98.67	98.74	96.99	1.0	1.0	10.7	11.2	2.8	3.3	4.6	3.5	31	37	52	39	42	na
XS5	59	98.65	98.51	96.79	1.1	1.1	11.7	13.3	2.9	3.3	4.6	3.4	39	44	61	46	31	na
XS6	45	97.82	97.80	95.81	1.1	1.2	11.8	13.6	2.8	3.4	4.9	3.5	38	46	66	48	45	na
XS7	34	97.43	97.28	95.16	1.1	1.2	10.7	13.2	3.1	3.8	5.1	3.8	41	50	67	51	36	na
XS8	16	95.90	96.05	95.16	1.0	1.1	9.9	11.1	2.7	3.3	4.6	3.4	30	36	51	38	48	na
XS9	0	95.63	95.75	92.93	1.3	1.5	14.0	20.9	3.8	4.3	6.8	4.2	80	89	142	87	--	na
												Average	43	49	72	51	[2]43	52
												stdev	16.9	18.3	31.9	17.1	7.1	12
												COV	0.40	0.37	0.44	0.34	na	0.24

[1]Spread is the percent difference between discharge computed with no expansion loss and discharge computed with full expansion loss, divided by the discharge computed with full expansion loss. Cross sections with spreads >1 are shown by --.

[2]This is the average energy balanced value for the reach given above that had the minimum spread of 0–1 percent.

Left Hand Creek at Buckingham Park

The indirect peak discharge (199 $m^3 s^{-1}$, tables 1 and 10) was measured on March 21, 2014, below the confluence of James and Left Hand Creeks. The main channel was scoured to bedrock along the upper cross sections (XS1–XS7, table 10) and had moderate to severe irregularities with minor obstructions (Manning's n=0.050 $m^{-1/3}$ s). There were more boulders in the bed of the lower reach (XS7–XS10, fig. 14). The left-bank flood plain had widely spaced (5–8 m) large trees (0.3- to 0.5-m diameter) with grass growing between the trees. For most of the reach, the left-bank, high-water mark was a distinct line were the grass changed from bent flat to standing upright. A separate indirect peak discharge measurement (225 $m^3 s^{-1}$) was made by John Pitlick, and based on velocity measurements made later and a one-dimensional flow model, he found Manning's n to be equal to 0.050 $m^{-1/3}$ s (University of Colorado, Geography Department, Boulder, Colo., written commun., 2015). The combined peak discharges in Left Hand Creek below Nugget Gulch and James Creek below Jamestown was 174 $m^3 s^{-1}$(table 1), which is less than the estimated peak below the confluence at Buckingham Park. The travel distance from the two upstream measurement sites to the confluence are about the same (1,400 m), but the difference in timing and attenuation effects should all combine to reduce the peak discharge below the confluence. The different indirect methods estimated that 79–86 percent of the flow was conveyed in the main channel (fig. 14), and the remainder was conveyed through the adjacent flood plains.

Figure 14. Left Hand Creek at Buckingham Park on March 21, 2014. View is upstream from cross section 10 (XS10, table 10) at the bottom of the measurement reach.

Table 10. Summary of indirect discharge measurements for Left Hand Creek at Buckingham Park, Boulder County, Colorado.

[ID, cross section identification; XS, cross section; LB, left bank; RB, right bank; HW, high-water mark; SAC, slope-area calculation; stdev, standard deviation; COV, coefficient of variation; m, meter; m^2, square meter; ms^{-1}, meter per second; $m^3\ s^{-1}$, cubic meter per second; na, not applicable]

ID	Distance from arbitrary zero (m)	Arbitrary elevation			Hydraulic radius (m)	Depth (m)	Width (m)	Area (m^2)	Mean cross-sectional velocity				Discharge					
		LB HW (m)	RB HW (m)	Thalweg (m)					Jarrett ($m\ s^{-1}$)	Cowan ($m\ s^{-1}$)	Empirical ($m\ s^{-1}$)	Critical flow ($m\ s^{-1}$)	Jarrett ($m^3\ s^{-1}$)	Cowan ($m^3\ s^{-1}$)	Empirical ($m^3\ s^{-1}$)	Critical flow ($m^3\ s^{-1}$)	SAC[1] ($m^3\ s^{-1}$)	Ensemble average ($m^3\ s^{-1}$)
XS1	137	99.99	99.72	96.60	2.0	2.2	20.7	45.4	4.4	5.5	7.8	4.9	198	250	353	223	--	na
XS2	124	99.46	99.67	96.19	1.8	1.9	24.0	46.5	4.3	5.2	6.2	4.7	200	244	288	220	--	na
XS3	113	99.51	99.34	95.74	1.9	2.1	24.0	50.2	4.4	5.4	6.4	4.8	219	272	324	243	--	na
XS4	102	98.78	99.21	95.23	1.2	1.2	35.3	43.3	4.1	5.0	5.9	4.5	176	217	254	195	--	na
XS5	84	98.67	98.84	95.35	2.0	2.2	21.3	47.4	4.5	5.5	6.4	5.0	212	260	306	235	--	na
XS6	67	98.21	98.54	95.30	1.8	1.9	20.9	40.4	4.2	5.0	5.8	4.6	170	202	234	185	126	na
XS7	52	97.84	98.05	95.09	1.6	1.7	21.0	36.4	3.8	4.8	5.8	4.4	137	177	212	162	201	na
XS8	38	97.28	97.77	94.57	1.7	1.8	19.6	35.4	3.7	4.8	5.2	4.4	131	169	183	154	133	na
XS9	21	97.20	97.49	94.13	1.8	1.9	20.9	40.2	4.0	5.0	6.1	4.5	161	203	244	182	--	na
XS10	0	96.96	97.03	93.98	1.6	1.7	22.0	37.9	3.7	4.6	5.5	4.2	142	175	207	159	--	na
												Average	175	217	261	196	[2]149	199
												stdev	32.1	37.7	55.3	32.9	41.4	42
												COV	0.18	0.17	0.21	0.17	na	0.21

[1]Spread is the percent difference between discharge computed with no expansion loss and discharge computed with full expansion loss, divided by the discharge computed with full expansion loss. Cross sections with spreads >1 are shown by --.

[2]This is the average energy balanced value for the reach given above that had the minimum spread of 0–1 percent.

Fourmile Canyon Creek at 491 Wagonwheel Gap

The indirect peak discharge (75 $m^3 s^{-1}$, tables 1 and 11) was measured on December 3, 2013, when the water was still unfrozen because the measurement site (fig. 15) is at a lower elevation (1,822 m) than most of the other sites. The upper basin of Fourmile Canyon Creek (drainage area 4.64 km^2) had previously been burned by the 2010 Fourmile Canyon fire. At this upper site (Fourmile Canyon Creek near Sunshine, Colo.; http://nwis.waterdata.usgs.gov/co/nwis/peak/?site_no=06730160&agency_cd=USGS), the U.S. Geological Survey's Colorado Water Science Center estimated a peak discharge of 31 $m^3 s^{-1}$±25 percent (R. Kimbrough, U.S. Geological Survey, written commun., 2015) with a unit peak discharge of 6.7 $m^3 s^{-1} km^{-2}$. At the measurement site (≈1,500 m downstream from the upper basin) the unit peak discharge decreased to 6.0 $m^3 s^{-1} km^{-2}$ (table 1), but the peak discharge more than doubled because of the band of high-accumulation, high-intensity rainfall (fig. 1) between it and the upper site. About 1 km downstream from the measurement site (Fourmile Canyon Creek at 491 Wagonwheel Gap) the channel leaves the mountains and spreads out onto an alluvial fan with several distributaries. An estimated peak discharge across this alluvial fan was 41.3 $m^3 s^{-1}$ (Wright Water Engineers, 2014, table ES–1). The site (Fourmile Canyon Creek at 491 Wagonwheel Gap) had a relatively wide flood plain along most of the right bank, but the flow (≈0.2 m deep) was through dense grass growing on the flood plain such that the different indirect methods estimated that 94–97 percent of the flow was conveyed in the main channel, and the remainder was conveyed through the adjacent flood plains.

Figure 15. Fourmile Canyon Creek at 491 Wagonwheel Gap on December 1, 2013. Upstream view from cross section 3 (XS3, table 10) at the bottom of the measurement reach.

Table 11. Summary of indirect discharge measurements for Fourmile Canyon Creek at 491 Wagonwheel Gap, Boulder County, Colorado.

[ID, cross section identification; XS, cross section; LB, left bank; RB, right bank; HW, high-water mark; SAC, slope-area calculation; stdev, standard deviation; COV, coefficient of variation; m, meter; m^2, square meter; ms^{-1}, meter per second; $m^3 s^{-1}$, cubic meter per second; na, not applicable]

ID	Distance from arbitrary zero (m)	Arbitrary elevation			Hydraulic radius (m)	Depth (m)	Width (m)	Area (m^2)	Mean cross-sectional velocity				Discharge					
		LB HW (m)	RB HW (m)	Thalweg (m)					Jarrett ($m\ s^{-1}$)	Cowan ($m\ s^{-1}$)	Empirical ($m\ s^{-1}$)	Critical flow ($m\ s^{-1}$)	Jarrett ($m^3\ s^{-1}$)	Cowan ($m^3\ s^{-1}$)	Empirical ($m^3\ s^{-1}$)	Critical flow ($m^3\ s^{-1}$)	SAC[1] ($m^3\ s^{-1}$)	Ensemble average ($m^3\ s^{-1}$)
XS1	48.5	100.37	100.35	98.75	0.9	0.9	15.4	14.5	2.4	4.2	5.1	3.3	34	60	74	47	--	na
XS2	37.7	99.76	99.65	97.82	1.0	1.0	16.4	16.9	2.5	4.1	5.1	3.2	42	69	86	54	--	na
XS3	26.5	99.18	99.54	97.05	1.1	1.2	15.1	18.3	3.2	5.3	7.2	3.9	58	97	131	72	70	na
XS4	18.5	98.65	99.38	96.67	1.1	1.2	13.9	17.1	3.4	5.6	7.6	4.1	57	95	130	69	65	na
XS5	0	97.78	98.03	95.2	1.3	1.5	10.7	16.0	3.3	5.7	7.9	4.1	53	92	126	66	80	na
												Average	49	82	109	62	[2]73	75
												stdev	10.5	16.8	27.4	10.6	8.0	23
												COV	0.21	0.20	0.25	0.17	na	0.30

[1]Spread is the percent difference between discharge computed with no expansion loss and discharge computed with full expansion loss, divided by the discharge computed with full expansion loss. Cross sections with spreads >1 are shown by --.

[2]This is the average energy balanced value for the reach given above that had the minimum spread of 0–1 percent.

Twomile Canyon Creek at 215 Linden

The indirect peak discharge (26 $m^3 s^{-1}$, tables 1 and 12) was measured on November 27, 2013. The measurement reach was a slot-like channel with only a vestige of a flood plain <1 m wide and the smallest width-to-depth ratio (3.4, table 1), but some of the largest boulders (D_{84} z-axis height=500 mm and D_{84} cross-stream axis=600 mm; fig. 16) of all the measurement sites. Wright Water Engineers (2014) reported 34 $m^3 s^{-1}$ at a site about 300 m downstream from Twomile Canyon Creek at 215 Linden. The unit peak discharge (7.7 $m^3 s^{-1} km^{-2}$, table 1) was the third largest because the average peak rainfall intensity was the second highest (49.0 mm h^{-1}; table 1 and fig. 1; 43.2 mm h^{-1}, table 7; Wright Water Engineers, 2014) of all the sites. The different indirect methods estimated that 88–93 percent of the flow was conveyed in the main channel (fig. 16). Flow from this channel immediately overflowed its bank once the channel exited the mountains about 200 m downstream and inundated Linden Avenue (see cover). Two people left a car caught in the rising water and debris from this stream on the evening of September 11–12, 2013, and were swept off Linden Avenue during the flood and died (Manzi, 2013).

Figure 16. Twomile Canyon Creek at 215 Linden on November 27, 2013. View is downstream from cross section 1 (XS1, table 11).

Table 12. Summary of indirect discharge measurements for Twomile Canyon Creek at 215 Linden, Boulder County, Colorado.

[ID, cross section identification; XS, cross section; LB, left bank; RB, right bank; HW, high-water mark; SAC, slope-area calculation; stdev, standard deviation; COV, coefficient of variation; m, meter; m^2, square meter; ms^{-1}, meter per second; $m^3 s^{-1}$, cubic meter per second; na, not applicable]

ID	Distance from arbitrary zero (m)	Arbitrary elevation			Hydraulic radius (m)	Depth (m)	Width (m)	Area (m^2)	Mean cross-sectional velocity				Discharge					
		LB HW (m)	RB HW (m)	Thalweg (m)					Jarrett ($m\ s^{-1}$)	Cowan ($m\ s^{-1}$)	Empirical ($m\ s^{-1}$)	Critical flow ($m\ s^{-1}$)	Jarrett ($m^3\ s^{-1}$)	Cowan ($m^3\ s^{-1}$)	Empirical ($m^3\ s^{-1}$)	Critical flow ($m^3\ s^{-1}$)	SAC[1] ($m^3\ s^{-1}$)	Ensemble average ($m^3\ s^{-1}$)
XS1	42	100.29	100.44	98.70	0.8	1.1	4.7	5.3	3.0	4.5	2.4	2.8	16.1	24.1	12.7	15.1	--	na
XS2	35	99.97	99.38	97.02	0.8	1.7	5.1	8.5	3.4	5.3	2.8	2.4	28.7	44.6	23.7	20.3	--	na
XS3	24	98.87	98.62	96.99	0.9	1.1	5.4	6.2	2.9	4.2	2.4	3.0	17.9	26.0	14.7	18.7	23.6	na
XS4	16	98.69	98.45	96.50	1.0	1.5	5.3	7.8	3.2	4.7	2.6	3.3	25.2	36.3	20.3	25.6	28.4	na
XS5	9	98.04	97.73	95.88	1.3	1.6	5.3	8.4	3.6	5.0	2.9	3.3	30.5	42.1	23.9	27.9	39.8	na
XS6	0	97.58	97.46	95.29	1.1	1.3	5.9	8.0	3.1	4.5	5.3	3.8	25.0	35.6	42.1	30.2	18.2	na
												Average	24	35	23	23	[2]27	26
												stdev	5.8	8.3	10.4	5.9	9.2	5.0
												COV	0.24	0.24	0.46	0.25	na	0.19

[1]Spread is the percent difference between discharge computed with no expansion loss and discharge computed with full expansion loss, divided by the discharge computed with full expansion loss. Cross sections with spreads >1 are shown by --.

[2]This is the average energy balanced value for the reach given above that had the minimum spread of 0–1 percent.

Fourmile Creek above Long Gulch

The indirect peak discharge (12 $m^3 s^{-1}$, tables 1 and 13) was measured on June 17, 2014. This site, at an elevation of about 2,300 m, was west of the high-accumulation, high-intensity rainfall band (fig. 1*C*) and, thus, experienced an average peak rainfall intensity of only 11.8 mm h^{-1} and had one of the lower peak runoff coefficients (0.16). This site was upstream from the area burned by the 2010 Fourmile Canyon fire (Ebel and others, 2012). The reach had a bend at XS4 (table 13) and a change in bed-material size (coarser upstream from bend) and a change in water-surface slope (0.054 upstream from the bend to 0.025 downstream from the bend) with slightly higher estimates of discharge at the cross sections above the bend than below the bend (table 13, fig. 17). Bed material was relatively small (table 1) and similar in size to the bed material of North St. Vrain Creek above the Highway 7 Bridge (also outside the high-accumulation, high-intensity rainfall band). Bedload estimates from equation 8 during the flood upstream from XS4 ranged from 190 to 390 kg $m^{-1} s^{-1}$ and 20 to 130 kg $m^{-1} s^{-1}$ downstream from XS4. Dense willows lined most of both banks (fig. 17); and the different indirect methods estimated that 84–93 percent of the flow was conveyed in the main channel, and the remainder was conveyed through the adjacent flood plains.

Figure 17. Fourmile Creek above Long Gulch on June 17, 2014. *A*, View is upstream from cross section 2 (XS2, table 13) and upstream from the bend at cross section 4 (XS4). *B*, View is upstream from cross section 9 (XS9, table 13) and downstream from the bend at XS4.

Table 13. Summary of indirect discharge measurements for Fourmile Creek above Long Gulch, Boulder County, Colorado.

[Highlighted cells represent the quality of the high-water mark. ID, cross section identification; XS, cross section; LB, left bank; RB, right bank; HW, high-water mark; SAC, slope-area calculation; stdev, standard deviation; COV, coefficient of variation; m, meter; m^2, square meter; ms^{-1}, meter per second; $m^3\ s^{-1}$, cubic meter per second; na, not applicable]

ID	Distance from arbitrary zero (m)	Arbitrary elevation			Hydraulic radius (m)	Depth (m)	Width (m)	Area (m^2)	Mean cross-sectional velocity				Discharge					
		LB HW (m)	RB HW (m)	Thalweg (m)					Jarrett ($m\ s^{-1}$)	Cowan ($m\ s^{-1}$)	Empirical ($m\ s^{-1}$)	Critical flow ($m\ s^{-1}$)	Jarrett ($m^3\ s^{-1}$)	Cowan ($m^3\ s^{-1}$)	Empirical ($m^3\ s^{-1}$)	Critical flow ($m^3\ s^{-1}$)	SAC[1] ($m^3\ s^{-1}$)	Ensemble average ($m^3\ s^{-1}$)
XS1	51	100.67	100.35	98.97	0.8	1.0	5.8	5.6	2.1	4.3	6.0	2.7	12	24	34	15	--	na
XS2	46	100.28	100.34	98.77	0.7	0.8	6.2	5.0	2.0	4.1	5.7	2.6	10	20	28	13	11	na
XS3	41	100.02	99.98	98.71	0.6	0.7	6.2	4.5	1.7	3.2	4.4	2.1	8	15	20	10	9	na
XS4	34	99.73	99.49	98.63	0.5	0.6	6.3	3.7	1.4	2.7	3.5	1.9	5	10	13	7	8	na
XS5	27	99.52	99.67	98.12	0.7	0.8	7.1	6.0	1.8	2.7	3.6	2.4	11	16	22	14	--	na
XS6	20	99.22	99.30	98.28	0.5	0.6	5.8	3.4	1.5	2.6	3.4	2.5	5	9	11	8	8	na
XS7	14	99.21	99.14	98.27	0.5	0.6	7.0	4.0	1.4	2.5	3.2	2.4	6	10	13	9	10	na
XS8	7	99.03	98.97	98.02	0.5	0.6	7.3	4.3	1.3	2.1	2.7	2.0	5	9	12	9	5	na
XS9	0	98.93	98.65	97.99	0.5	0.5	8.3	4.4	1.1	1.9	2.3	1.8	5	8	10	8	9	na
		Good										**Average**	7.3	13	18	10	[2]8.4	12
		Fair										**stdev**	2.7	5.6	8.4	3.0	1.7	4.3
		Poor										**COV**	0.37	0.42	0.47	0.29	na	0.38
		Very poor																

[1]Spread is the percent difference between discharge computed with no expansion loss and discharge computed with full expansion loss, divided by the discharge computed with full expansion loss. Cross sections with spreads >1 are shown by --.

[2]This is the average energy balanced value for the reach given above that had the minimum spread of 0–1 percent.

Long Gulch above Loretta-Linda

The indirect peak discharge (16 $m^3 s^{-1}$, tables 1 and 14) was measured on June 25, 2014. Long Gulch is usually an intermittent stream that often dries up during the summer but continued to flow during the summer of 2014. The west-facing slopes of Long Gulch (fig. 1*B*) drain part of the area burned by the 2010 Fourmile Canyon fire (Ebel and others, 2012), whereas the east-facing slopes were unburned. Loretta-Linda refers to an unamed tributary downstream from this measurement site that drains a small basin (Loretta-Linda at flume 9–1, 0.39 km^2, table 1) severely burned by the 2010 Fourmile Canyon fire. The different indirect methods estimated that 87–94 percent of the flow was conveyed in the main channel with the remainder flowing overbank on the right side of the channel (fig. 18).

Figure 18. Long Gulch above Loretta-Linda on June 25, 2014. View is upstream from about cross section 7 (XS7, table 14). Photograph taken by J. Smith, III.

Table 14. Summary of indirect discharge measurements for Long Gluch above Loretta-Linda, Boulder County, Colorado.

[Highlighted cells represent the quality of the high-water mark. ID, cross section identification; XS, cross section; LB, left bank; RB, right bank; HW, high-water mark; SAC, slope-area calculation; stdev, standard deviation; COV, coefficient of variation; m, meter; m^2, square meter; ms^{-1}, meter per second; $m^3\ s^{-1}$, cubic meter per second; na, not applicable]

ID	Distance from arbitrary zero (m)	Arbitrary elevation			Hydraulic radius (m)	Depth (m)	Width (m)	Area (m^2)	Mean cross-sectional velocity				Discharge					
		LB HW (m)	RB HW (m)	Thalweg (m)					Jarrett ($m\ s^{-1}$)	Cowan ($m\ s^{-1}$)	Empirical ($m\ s^{-1}$)	Critical flow ($m\ s^{-1}$)	Jarrett ($m^3\ s^{-1}$)	Cowan ($m^3\ s^{-1}$)	Empirical ($m^3\ s^{-1}$)	Critical flow ($m^3\ s^{-1}$)	SAC[1] ($m^3\ s^{-1}$)	Ensemble average ($m^3\ s^{-1}$)
XS1	43	102.33	102.32	101.01	0.7	0.9	4.8	4.2	2.2	5.7	7.4	3.2	10	24	31	13	--	na
XS2	37	101.67	101.61	100.25	0.7	1.0	4.4	4.5	2.6	6.1	8.3	3.4	11	28	37	15	--	na
XS3	29	101.55	101.40	99.83	0.7	0.9	6.1	5.7	2.6	6.2	8.3	3.4	15	35	47	19	22	na
XS4	23	100.60	100.70	99.49	0.7	0.8	5.5	4.3	2.2	5.1	6.5	3.0	9	22	28	13	18	na
XS5	17	100.23	100.29	99.24	0.6	0.6	6.3	3.9	2.1	4.3	5.4	2.8	8	17	21	11	14	na
XS6	12	99.93	99.93	98.64	0.5	0.6	6.6	3.9	2.1	5.0	6.4	2.9	8	19	25	11	16	na
XS7	4	99.63	99.16	98.34	0.6	0.7	3.9	2.7	1.9	4.7	5.9	2.8	5	13	16	8	8.5	na
XS8	0	99.01	98.85	97.74	0.5	0.7	3.0	2.1	1.7	5.0	5.8	2.9	4	10	12	6	7.7	na
												Average	9	21	27	12	[2]12	16
												stdev	3.5	8.0	11.4	4.2	5.5	7.7
												COV	0.40	0.38	0.42	0.35	na	0.48

Good
Fair
Poor
Very poor

[1]Spread is the percent difference between discharge computed with no expansion loss and discharge computed with full expansion loss, divided by the discharge computed with full expansion loss. Cross sections with spreads >1 are shown by --.

[2]This is the average energy balanced value for the reach given above that had the minimum spread of 0–1 percent.

Loretta-Linda at Flume 9–1

The indirect peak discharge (6.3 $m^3 s^{-1}$, tables 1 and 15) was measured on July 7, 2014 at the mouth of the Loretta-Linda basin severely burned by the 2010 Fourmile Canyon fire. This is an ephemeral channel. A 9-inch wide, modified Parshall flume (Kilpatrick and Schneider, 1983) was installed to measure runoff from the basin during 2011. Runoff from a summer convective storm on July 13, 2011 (10-min peak rainfall intensity=52.1 mm h^{-1}), completely filled this flume with sediment such that an indirect peak discharge measurement was made at this site in 2011. Average peak discharge (assuming critical flow at two cross sections) was 4.6 $m^3 s^{-1}$, and the unit peak discharge was 12 $m^3 s^{-1} km^{-2}$ (U.S. Geological Survey, Boulder, Colo., unpub data) similar to the unit peak discharge (16.2 $m^3 s^{-1} km^{-2}$) for the September 2013 storms associated with an average peak rainfall intensity of 51.0 mm h^{-1} (table 1). Whereas the high-water marks for the 2011 flood were on the order of 0.2–0.8 m higher than the September 2013 high-water marks at XS4 and XS5, the channel bed had scoured during the 2013 floods by about 0.5 to 1.5 m. The different indirect methods estimated that 88–97 percent of the flow was conveyed in the main channel with the remainder flowing overbank on both sides of the channel (fig. 19).

Figure 19. Loretta-Linda at flume 9–1 on July 7, 2014. View is downstream from cross section 1 (XS1, table 15) at the old site for the flume.

Table 15. Summary of indirect discharge measurements for Loretta-Linda at flume 9-1, Boulder County, Colorado.

[Highlighted cells represent the quality of the high-water mark. ID, cross section identification; XS, cross section; LB, left bank; RB, right bank; HW, high-water mark; SAC, slope-area calculation; stdev, standard deviation; COV, coefficient of variation; m, meter; m^2, square meter; ms^{-1}, meter per second; $m^3\ s^{-1}$, cubic meter per second; na, not applicable]

ID	Distance from arbitrary zero (m)	Arbitrary elevation			Hydraulic radius (m)	Depth (m)	Width (m)	Area (m^2)	Mean cross-sectional velocity				Discharge					
		LB HW (m)	RB HW (m)	Thalweg (m)					Jarrett ($m\ s^{-1}$)	Cowan ($m\ s^{-1}$)	Empirical ($m\ s^{-1}$)	Critical flow ($m\ s^{-1}$)	Jarrett ($m^3\ s^{-1}$)	Cowan ($m^3\ s^{-1}$)	Empirical ($m^3\ s^{-1}$)	Critical flow ($m^3\ s^{-1}$)	SAC[1] ($m^3\ s^{-1}$)	Ensemble average ($m^3\ s^{-1}$)
XS1	20	101.17	100.76	99.96	0.45	0.54	4.95	2.68	2.1	3.9	6.2	2.9	5.7	10	17	7.8	--	na
XS2	16	99.92	99.92	98.90	0.48	0.63	3.10	1.95	1.9	4.1	7.6	2.8	3.7	8.0	15	5.5	8.3	na
XS3	12	99.32	99.39	98.26	0.34	0.57	1.96	1.12	1.9	4.3	7.7	2.8	2.2	4.8	8.6	3.2	3.4	na
XS4	10	99.18	99.26	98.23	0.32	0.64	2.48	1.60	1.4	4.6	6.9	3.0	2.3	7.3	11	4.8	3.9	na
XS5	7.1	98.69	98.80	98.04	0.35	0.43	2.86	1.23	1.4	3.0	4.8	2.2	1.7	3.7	5.9	2.7	3.0	na
XS6	4	98.64	98.66	97.68	0.40	0.47	3.80	1.78	1.7	3.5	6.1	2.4	3.0	6.2	11	4.3	2.8	na
XS7	0	98.34	98.18	97.36	0.46	0.52	5.02	2.62	1.8	3.7	6.8	2.6	4.8	10	18	6.7	3.4	na
		Good										**Average**	3.3	7.2	12	5.0	[2]3.9	6.3
		Fair										**stdev**	1.5	2.5	4.3	1.8	2.1	3.6
		Poor										**COV**	0.44	0.35	0.35	0.37	na	0.57
		Very poor																

[1]Spread is the percent difference between discharge computed with no expansion loss and discharge computed with full expansion loss, divided by the discharge computed with full expansion loss. Cross sections with spreads >1 are shown by --.

[2]This is the average energy balanced value for the reach given above that had the minimum spread of 0–1 percent.

Sugarloaf

The indirect peak discharge (0.057 $m^3 s^{-1}$, tables 1 and 16) was measured on June 2, 2015. This was a first-order ephemeral channel draining a small basin (0.0084 km^2) on a north-facing hillslope severely burned by the 2010 Fourmile Canyon fire (Ebel and others, 2012). The channel had been scoured and enlarged by a succession of floods (measured with a 3-inch wide, modified Parshall flume) produced by summer convective storms in 2010, 2011, and 2012; for example, the peak discharge for a storm on July 10, 2011 (2-min, maximum rainfall intensity of 45.8 mm h^{-1}), was 0.046 $m^3 s^{-1}$or 5.5 $m^3 s^{-1} km^{-2}$. Channel cross-sections for the first indirect peak discharge measurement were extracted from tripod mounted light and detection ranging (lidar) data collected on September 22, 2013 but unfortunately were unable to sufficiently resolve the small channel with widths of 1–2 m and depths on the order of 0.1 m. The standard method described in the "Field Methods" section was, therefore, used to remeasure the cross sections on June 2, 2015.

Methods used for the perennial, lower gradient streams (Cowan, Jarrett, Empirical, Critical flow, and SA) were inappropriate for this hillslope channel with the steepest mean bed slope (0.37) and a series of steps and pools caused by roots and large stones; therefore, two methods (Yochum and Comiti) developed for step-pool mountain streams with steep bed slopes (up to 0.37) were applied in addition to using the measured value of Manning's *n* (0.21 $m^{-1/3}$ s; see Measured "*n*" method above), and the Critical Flow method.

Peak discharges estimates for the lowest two cross sections (XS1 and XS2, table 16) were quite different than for the upper six cross sections (XS3–XS8). No obvious tributary entered the channel downstream from the upper six cross sections (fig. 20), which might explain the increase in flow. The characteristics of the channel appear to change downstream from the upper six cross sections. The cross-sectional area and mean velocities are different, and the average relative submergence (R/D_{84}) was 1.1 and 0.7 for XS1 and XS2, respectively, which is more characteristic of the other sites for which R/D_{84} was always >1. For the upper six cross sections, R/D_{84} ranged from 0.4 to 0.8, which is typical of the step-pool type channels used to develop the Yochum and Comiti methods. Using all eight cross sections gives an ensemble average of 0.12 $m^3 s^{-1}$ (unit peak discharge=14.2 $m^3 s^{-1} km^{-2}$) and a physically unrealistic peak runoff coefficient of 1.1. It appears XS1 and XS2 are outliers compared to the upper six cross sections, and perhaps the high-water marks for these XS1 and XS2 were incorrect. For such relatively small cross-sectional areas (table 16), a change in the elevation of the high-water mark can represent a substantial change in peak discharge. Lowering the estimated high-water elevation at XS1 and XS2 by 0.05 m reduces the peak discharge estimates by 40–60 percent. For these reasons, the estimate peak discharge for this site was based on the six upper cross sections. This value given above (0.057 $m^3 s^{-1}$) is also similar to the indirect peak discharge of the convective storm in 2011 in response to similar rainfall intensities (45.8 and 45.7 mm h^{-1} for the convective storm and September 2013 storms, respectively). All flow was within the main channel because no flood plain existed.

Figure 20. Sugarloaf on September 22, 2013. View is upstream from cross section 2 (XS2, table 16). The upper six cross sections extend from cross section 3 (high-water elevation line) to just downstream of the black log directly up the channel.

Table 16. Summary of indirect discharge measurements for Sugarloaf, Boulder County, Colorado.

[The value of standard deviation of the vertical bed elevations of a longitudinal profile (measured every 0.05 m), σ_z, was 0.054 m. ID, cross section identification; θ, local slope angle where the sine of the angle was equal to the change in elevation over the distance from a point one-half of a channel width downstream to a point one-half of a channel width upstream from the cross section divided by the distance parallel to the slope between the two points; XS, cross section; LB, left bank; RB, right bank; HW, high-water mark; SAC, slope-area calculation; stdev, standard deviation; COV, coefficient of variation; m, meter; m^2, square meter; ms^{-1}, meter per second; $m^3 s^{-1}$, cubic meter per second; na, not applicable]

ID	Local sin Θ	Slope distance from XS1 (m)	Arbitrary elevation			Hydraulic radius (m)	Depth (m)	Width (m)	Area (m^2)	Mean cross-sectional velocity				Discharge				
			LB HW (m)	RB HW (m)	Thalweg (m)					Measured 'n' ($m\ s^{-1}$)	Yochum ($m\ s^{-1}$)	Comiti ($m\ s^{-1}$)	Critical flow ($m\ s^{-1}$)	Measured 'n' ($m^3\ s^{-1}$)	Yochum ($m^3\ s^{-1}$)	Comiti ($m^3\ s^{-1}$)	Critical flow ($m^3\ s^{-1}$)	Ensemble average ($m^3\ s^{-1}$)
XS1	0.36	0	2292.43	2292.44	2292.11	0.11	0.15	1.40	0.21	1.0	1.6	3.2	1.4	0.21	0.33	0.66	0.29	na
XS2	0.46	2.13	2293.12	2293.08	2292.83	0.08	0.09	2.26	0.20	0.8	0.9	1.4	1.1	0.17	0.19	0.28	0.23	na
XS3	0.35	3.35	2293.76	2293.77	2293.61	0.04	0.04	2.19	0.091	0.5	0.3	0.4	0.8	0.043	0.029	0.039	0.073	na
XS4	0.19	11.89	2297.40	2297.28	2297.18	0.06	0.07	0.98	0.073	0.4	0.4	0.7	1.0	0.032	0.026	0.050	0.070	na
XS5	0.56	14.02	2297.94	2297.90	2297.79	0.06	0.07	1.04	0.070	0.6	0.6	0.6	0.6	0.044	0.028	0.027	0.059	na
XS6	0.23	15.24	na	2298.32	2298.13	0.08	0.09	0.83	0.075	0.5	0.5	0.9	1.0	0.040	0.037	0.069	0.078	na
XS7	0.31	17.07	na	2298.34	2298.17	0.07	0.07	0.85	0.063	0.6	0.5	0.9	1.0	0.037	0.034	0.054	0.063	na
XS8	0.17	19.20	2299.38	2299.31	2299.14	0.10	0.11	1.08	0.12	0.5	0.5	0.5	0.5	0.062	0.071	0.17	0.14	na
											XS1–XS8		**Average**	0.079	0.09	0.17	0.12	0.12
													stdev	0.068	0.11	0.22	0.09	0.040
													COV	0.86	1.19	1.28	0.70	0.34
											XS3–XS8		**Average**	0.043	0.038	0.069	0.080	0.057
													stdev	0.010	0.017	0.053	0.028	0.020
													COV	0.24	0.45	0.77	0.35	0.35

Fourmile Creek at Logan Mill

The indirect peak discharge (67 $m^3 s^{-1}$, tables 1 and 17) was measured on September 22, 2013. This site had a narrow (1–2 m) flood plain along the left bank with trees and bushes, a wider (3–8 m) flood plain along the right bank covered with grass, and a main channel at low flow that was 6–7 m wide (fig. 21). For the Cowan and SA methods, Manning's *n* was equal to 0.060 $m^{-1/3}$ s for the left-bank flood plain, 0.043 $m^{-1/3}$ s for the main channel, and 0.050 $m^{-1/3}$ s for the right-bank flood plain (fig. 21). An indirect estimate made by the U.S. Geological Survey Colorado Water Science Center for this site was 58 $m^3 s^{-1}$ ±15 to 25 percent (R. Kimbrough, written commun.; http://nwis.waterdata.usgs.gov/co/nwis/peak/?site_no=06727410&agency_cd=USGS) and another estimate of 53 $m^3 s^{-1}$ was made by Ritsch and others (2013) using the flow simulation Hydrologic Engineering Center's River Analysis System (HEC–RAS) model. The lower value estimated by Ritsch and others (2013) reflects the different values of Manning's *n* (0.05 $m^{-1/3}$ s for the main channel and 0.08 $m^{-1/3}$ s for the flood plains). The Urban Drainage and Flood Control Districts lists a peak discharge of 65 $m^3 s^{-1}$ for the site Fourmile Creek d/s Poorman Rd upstream from #1267 Fourmile Cr Rd nr Orodell (http://alert5.udfcd.org/wp/?page_id=115, accessed August 3, 2015), which is about 2,000 m downstream from Fourmile Creek at Logan Mill. With definite flood plains on both sides, the different indirect methods estimated that 73–86 percent of the flow was conveyed in the main channel with the remainder across the flood plain (fig. 21).

Figure 21. Fourmile Creek at Logan Mill on September 22, 2013. View is upstream from cross section 2 (XS2, table 17).

Table 17. Summary of indirect discharge measurements for Fourmile Creek at Logan Mill, Boulder County, Colorado.

[Highlighted cells represent the quality of the high-water mark. ID, cross section identification; XS, cross section; LB, left bank; RB, right bank; HW, high-water mark; SAC, slope-area calculation; stdev, standard deviation; COV, coefficient of variation; m, meter; m^2, square meter; ms^{-1}, meter per second; $m^3\ s^{-1}$, cubic meter per second; na, not applicable]

ID	Distance from arbitrary zero (m)	Arbitrary elevation			Hydraulic radius (m)	Depth (m)	Width (m)	Area (m^2)	Mean cross-sectional velocity				Discharge					
		LB HW (m)	RB HW (m)	Thalweg (m)					Jarrett ($m\ s^{-1}$)	Cowan ($m\ s^{-1}$)	Empirical ($m\ s^{-1}$)	Critical flow ($m\ s^{-1}$)	Jarrett ($m^3\ s^{-1}$)	Cowan ($m^3\ s^{-1}$)	Empirical ($m^3\ s^{-1}$)	Critical flow ($m^3\ s^{-1}$)	SAC[1] ($m^3\ s^{-1}$)	Ensemble average ($m^3\ s^{-1}$)
XS 1	0.0	6.68	7.02	5.24	0.9	0.9	11.3	10.5	2.7	4.5	4.9	3.4	28	47	51	36	--	na
XS 2	15.9	7.61	7.89	5.77	0.8	0.9	14.9	13.0	2.6	4.9	5.3	3.5	34	64	68	45	76	na
XS 3	31.2	7.98	7.90	5.28	1.0	1.1	18.6	19.8	3.4	5.3	6.0	3.9	66	105	118	78	103	na
XS 4	41.1	8.41	8.13	6.07	1.0	1.0	17.4	18.1	3.1	5.3	6.0	3.8	56	97	109	69	23	na
XS 5	56.4	8.76	8.95	6.45	1.2	1.3	15.8	20.3	3.2	5.2	5.8	3.8	66	105	117	78	53	na
		Good										**Average**	50	83	93	61	[2]49	67
		Fair										**stdev**	18.0	26.4	31.0	19.6	33.9	20
		Poor										**COV**	0.36	0.32	0.33	0.32	na	0.23
		Very poor																

[1]Spread is the percent difference between discharge computed with no expansion loss and discharge computed with full expansion loss, divided by the discharge computed with full expansion loss. Cross sections with spreads >1 are shown by --.

[2]This is the average energy balanced value for the reach given above that had the minimum spread of 0–1 percent.

Boulder Creek at Mouth of Boulder Canyon

The indirect peak discharge (109 $m^3 s^{-1}$, tables 1 and 18) was measured on March 14 and 16, 2014. The right bank of this reach was revetment consisting of blasted granite boulders used to protect Highway 119 in Boulder Canyon (fig. 1*B* and fig. 22). The left bank was a variety of stones and stonework built to protect Canon Park, a road providing access to homes at the mouth of the Boulder Canyon. This reach had some of the largest bed elements, but the spacing between elements produced relatively empty "gaps" that occupied about 28 percent of the bed (fig. 22), and the bed in this reach most resembled Rock Creek near Darby, Montana (Barnes, 1967). This measurement site had the lowest coefficient of variation reflecting the relative uniform channel properties (table 18). Because the flow was confined by protective material along each bank, the different indirect methods estimated that 91–94 percent of the flow was conveyed in the main channel. The Urban Drainage and Flood Control District lists a peak discharge of 107 $m^3 s^{-1}$ for their site, 4420 Bridge, about 1,500 m upstream from Boulder Creek at Mouth of Canyon (http://alert5.udfcd.org/wp/?page_id=115, accessed August 3, 2015).

Figure 22. Boulder Creek at mouth of Boulder Canyon on March 16, 2014. View is upstream from cross section 9 (XS9, table 18). Highway 119 begins in the upper left and passes the yellow highway sign.

Table 18. Summary of indirect discharge measurements for Boulder Creek at mouth of Boulder Canyon, Boulder County, Colorado.

[ID, cross section identification; XS, cross section; LB, left bank; RB, right bank; HW, high-water mark; SAC, slope-area calculation; stdev, standard deviation; COV, coefficient of variation; m, meter; m^2, square meter; ms^{-1}, meter per second; $m^3 s^{-1}$, cubic meter per second; na, not applicable]

ID	Distance from arbitrary zero (m)	Arbitrary elevation			Hydraulic radius (m)	Depth (m)	Width (m)	Area (m^2)	Mean cross-sectional velocity				Discharge					
		LB HW (m)	RB HW (m)	Thalweg (m)					Jarrett ($m\ s^{-1}$)	Cowan ($m\ s^{-1}$)	Empirical ($m\ s^{-1}$)	Critical flow ($m\ s^{-1}$)	Jarrett ($m^3\ s^{-1}$)	Cowan ($m^3\ s^{-1}$)	Empirical ($m^3\ s^{-1}$)	Critical flow ($m^3\ s^{-1}$)	SAC[1] ($m^3\ s^{-1}$)	Ensemble average ($m^3\ s^{-1}$)
XS1	133	100.02	99.92	97.78	1.5	1.6	21.1	33.4	2.9	2.8	4.0	3.5	97	94	133	119	--	na
XS2	114	99.76	99.52	97.64	1.4	1.4	21.5	30.5	2.8	2.8	3.6	3.5	84	85	111	107	--	na
XS3	99	99.08	99.20	96.86	1.5	1.5	17.8	27.4	2.9	2.9	4.0	3.6	80	79	109	98	--	na
XS4	87	99.33	99.28	96.54	1.8	1.9	18.5	36.0	3.7	3.5	5.3	4.2	132	126	189	151	--	na
XS5	76.5	98.26	98.37	95.51	1.3	1.4	21.1	29.0	3.2	3.3	4.6	4.1	94	95	135	118	--	na
XS6	58	98.31	98.56	95.35	1.6	1.8	18.1	33.1	3.5	3.4	5.0	4.0	114	112	165	133	65	na
XS7	43	97.74	98.09	95.61	1.5	1.7	17.8	30.6	3.3	3.3	4.7	4.1	102	100	143	125	111	na
XS8	30	97.21	97.30	95.02	1.6	1.8	17.7	31.2	3.2	3.1	4.4	3.8	98	97	136	119	131	na
XS9	14	96.79	96.99	94.71	1.5	1.6	19.7	32.5	3.0	2.9	4.1	3.6	97	95	132	116	87	na
XS10	0	96.21	96.79	94.08	1.5	1.6	17.7	28.8	2.9	2.9	4.0	3.5	84	83	115	101	75	na
												Average	98	97	137	119	[2]92	109
												stdev	16.4	14.8	26.2	16.5	27.2	19
												COV	0.17	0.15	0.19	0.14	na	0.17

[1]Spread is the percent difference between discharge computed with no expansion loss and discharge computed with full expansion loss, divided by the discharge computed with full expansion loss. Cross sections with spreads >1 are shown by --.

[2]This is the average energy balanced value for the reach given above that had the minimum spread of 0–1 percent.

Gregory Creek below Long Canyon

The indirect peak discharge (17 $m^3 s^{-1}$, tables 1 and 19) was measured on May 28, 2014. The "torturous" character of the channel made any relatively straight reach short, and additionally, the upper reach had several waterfalls; thus, only four cross sections could be measured, and these had the largest roughness elements of any site (D_{84}, *z-axis*=500 mm and $D_{84,}$ cross-stream axis =900 mm). Manning's *n* in the main channel was chosen to be 0.18 $m^{-1/3}$ s based on the resemblance to photographs of East St. Louis Creek reach ESL7 (cascade, n=0.17 $m^{-1/3}$ s) and ESL1 (step pool, n=0.19 $m^{-1/3}$ s) published by Yochum and Bledsoe (2010). Along the channel margins, Manning's *n* was chosen to be 0.25 $m^{-1/3}$ s (fig. 23). The mean water-surface slope was 0.099, whereas the mean bed slope was 0.065 (table 1). In this steep part of the canyon there was essentially no flood plain. Consequently, the different indirect methods estimated that 94–98 percent of the flow was conveyed in the main channel, and the remainder was conveyed through the heavy bush and boulders along the banks.

Figure 23. Gregory Creek below Long Canyon on December 2, 2013. View is downstream from cross section 3 (XS3, table 19 upper).

Table 19. Summary of indirect discharge measurements for Gregory Creek, Boulder County, Colorado.

[Highlighted cells represent the quality of the high-water mark. ID, cross section identification; XS, cross section; LB, left bank; RB, right bank; HW, high-water mark; SAC, slope-area calculation; stdev, standard deviation; COV, coefficient of variation; m, meter; m^2, square meter; ms^{-1}, meter per second; $m^3\ s^{-1}$, cubic meter per second; na, not applicable]

ID	Distance from arbitrary zero (m)	Arbitrary elevation			Hydraulic radius (m)	Depth (m)	Width (m)	Area (m^2)	Mean cross-sectional velocity				Discharge					
		LB HW (m)	RB HW (m)	Thalweg (m)					Jarrett ($m\ s^{-1}$)	Cowan ($m\ s^{-1}$)	Empirical ($m\ s^{-1}$)	Critical flow ($m\ s^{-1}$)	Jarrett ($m^3\ s^{-1}$)	Cowan ($m^3\ s^{-1}$)	Empirical ($m^3\ s^{-1}$)	Critical flow ($m^3\ s^{-1}$)	SAC[1] ($m^3\ s^{-1}$)	Ensemble average ($m^3\ s^{-1}$)
Gregory Creek below Long Canyon																		
XS1	21	101.34	101.41	99.44	0.8	1.0	7.3	7.1	2.4	1.9	4.6	3.3	17	14	33	23	--	na
XS2	14	100.68	100.62	98.74	1.0	1.3	5.9	7.5	2.9	2.1	5.6	3.4	22	16	42	26	13	na
XS3	7	99.79	99.84	98.66	0.7	0.8	6.4	5.4	2.1	1.6	3.3	2.8	11	9	18	15	11	na
XS4	0	99.40	99.31	97.96	0.7	0.8	7.4	6.1	2.1	1.7	3.5	3.0	13	10	22	18	7	na
												Average	16	12	29	21	10	17
												stdev	4.7	3.3	11.0	4.7	3.2	7.4
												COV	0.30	0.27	0.39	0.23	na	0.43
Gregory Creek at Rest Area																		
XS1	31	101.96	102.11	100.75	0.8	0.9	11.2	9.6	2.3	3.5	4.9	3.1	22	33	47	29	--	na
XS2	21	101.37	101.52	99.95	0.9	1.0	9.4	9.4	2.6	4.0	6.2	3.4	24	38	58	32	36	na
XS3	12	101.10	101.08	99.06	1.1	1.2	10.3	12.5	3.4	4.4	6.1	3.9	42	55	76	49	44	na
XS4	0	99.94	99.97	98.53	0.9	1.0	11.5	11.5	2.7	3.9	5.9	3.4	31	45	68	38	42	na
		Good										**Average**	30	43	62	37	[2]41	43
		Fair										**stdev**	8.9	9.5	12.8	8.8	4.3	12
		Poor										**COV**	0.30	0.22	0.21	0.24	na	0.28
		Very poor																

[1]Spread is the percent difference between discharge computed with no expansion loss and discharge computed with full expansion loss, divided by the discharge computed with full expansion loss. Cross sections with spreads >1 are shown by --.

[2]This is the average energy balanced value for the reach given above that had the minimum spread of 0–1 percent.

Gregory Creek at Rest Area

The indirect peak discharge (43 $m^3 s^{-1}$, tables 1 and 19) was measured on May 28, 2014. This reach of the channel, Gregory Creek at Rest Area, had a different character than Gregory Creek below Long Canyon. The mean water-surface slope (0.065) was similar to the mean bed slope (0.073). The reach was broader (table 19) with grass covering boulders. Several large willow trees were in the channel (fig. 24), but their wakes probably did not overlap during high flow. These were estimated to occupy <15 percent of the channel so that Manning's *n* was selected to be 0.070 $m^{-1/3}$ s (Arcement and Schneider, 1992, table 1). The Manning's *n* for the banks was 0.075 $m^{-1/3}$ s. These *n* values are quite different than for the measurement site Gregory Creek below Long Canyon. Two unnamed tributaries (along Crown Rock trail and Saddle Rock trail) increase the drainage area below Long Canyon by about 25 percent and contributed an unknown discharge to that measured upstream at Gregory Creek below Long Canyon but probably not enough to explain the increase from 17 $m^3 s^{-1}$ to 43 $m^3 s^{-1}$.

The peak runoff coefficient for this site was 1.0, which seems physically unrealistic. The average peak rainfall intensity (37.5 mm h^{-1}) is essentially the same as the 30-min value (38.6 mm h^{-1}) given for Gregory Creek west subwatershed reported by Wright Water Engineers (2014) in their table 6. The original estimate of *n* for the large willow trees with their associated debris (fig. 24) may be incorrect. If the *n* value for the main channel is increased by 20 percent to n=0.084 $m^{-1/3}$ s, then the ensemble average peak discharge only decreases from 43 to 41 $m^3 s^{-1}$, and the peak runoff coefficient is essentially unchanged. Another possibility is that the high-water marks are incorrect and too high. Lowering the elevation of the high-water marks by 0.1 m reduced the ensemble average peak discharge to 35 $m^3 s^{-1}$ and the peak runoff coefficient to 0.92. The different indirect methods estimated that 75–87 percent of the flow was conveyed in the main channel with the remainder through the grass and shrubs along the banks.

Figure 24. Gregory Creek at Rest Area on December 2, 2013. View is downstream from cross section 3 (XS3, table 19 lower).

Bluebell Canyon Creek above Mesa Trail Crossing

The indirect peak discharge (95 $m^3 s^{-1}$, tables 1 and 20) was measured on June 6, 2014, and was probably a debris flow not a fluid flow. Initial ensemble average peak discharge assuming a fluid flow (that is, using the Cowan, Jarrett, Empirical, and Critical flow methods) was 318 $m^3 s^{-1}$ (table 20) and the peak runoff coefficient was much greater than 1 suggesting that this flow was probably a debris flow. The channel reach had smooth sides (no flood plain) in sedimentary rock outcrops and relatively little sediment on the channel bed (fig. 25*A*) compared to other measurement sites. The steep side-wall provided no location for the deposition of characteristic levees that could be used to identify the flow as a debris flow; however, downstream from Mesa Trail Crossing was an extensive deposit of sediment (fig. 25*B*). Assuming the flow was a debris flow, the Bagnold method gave a peak flow of 95 $m^3 s^{-1}$ and unit peak discharge of 226 $m^3 s^{-1} km^{-2}$ (table 1; fig. 25*C*). Because this was probably a debris flow, no peak runoff coefficient is listed in table 1.

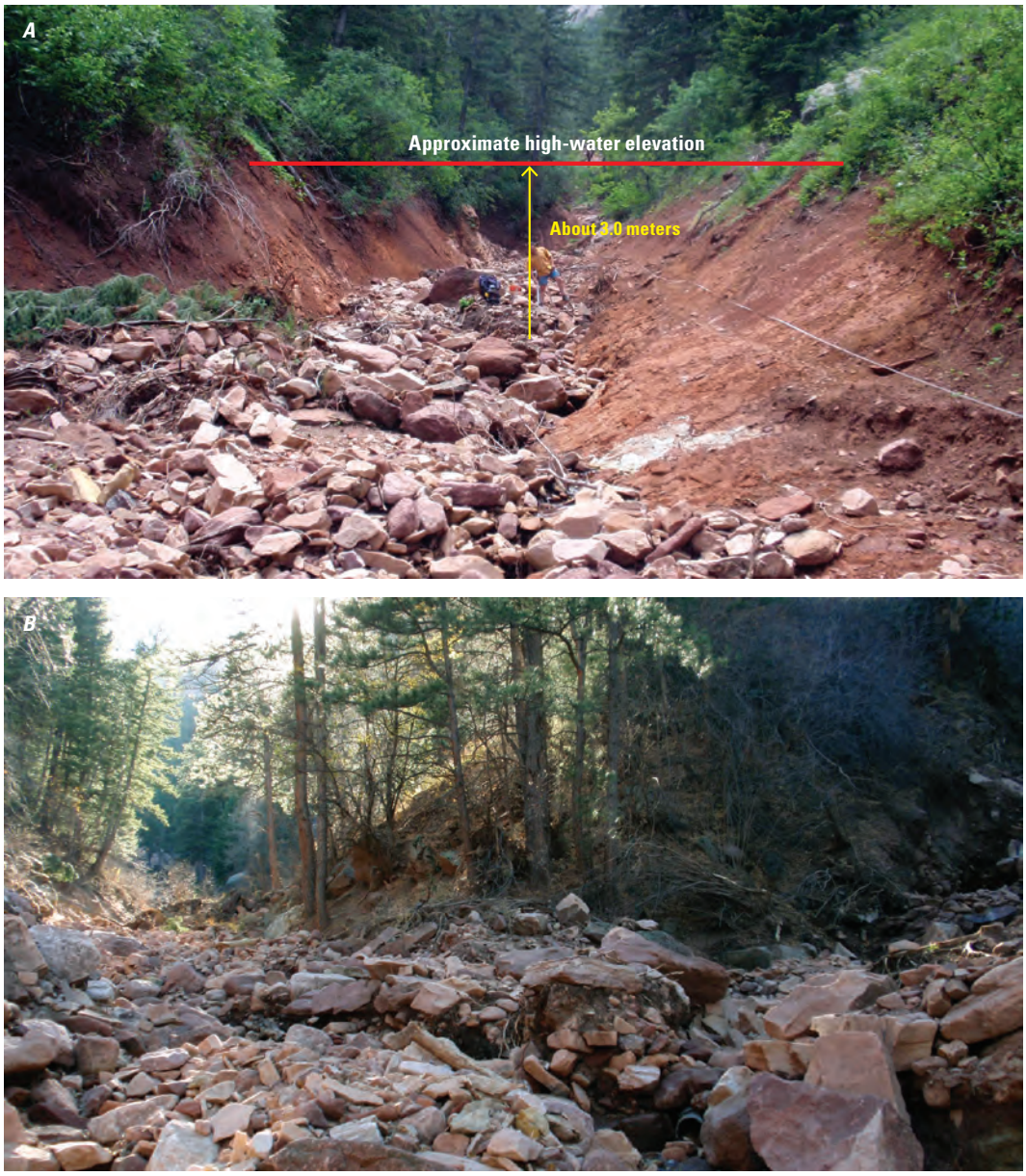

Figure 25. Bluebell Canyon Creek above Mesa Trail Crossing. *A*, View is upstream from cross section 1 (XS1, table 20) on June 6, 2014. *B*, View is upstream of debris deposited downstream from Mesa Trail Crossing. Photograph taken on November 10, 2013. *C*, The Bluebell Canyon Creek debris flow among debris flows generated from other burned areas. [$m^3 s^{-1} km^{-2}$, cubic meter per second per square kilometer; km^2, square kilometer]

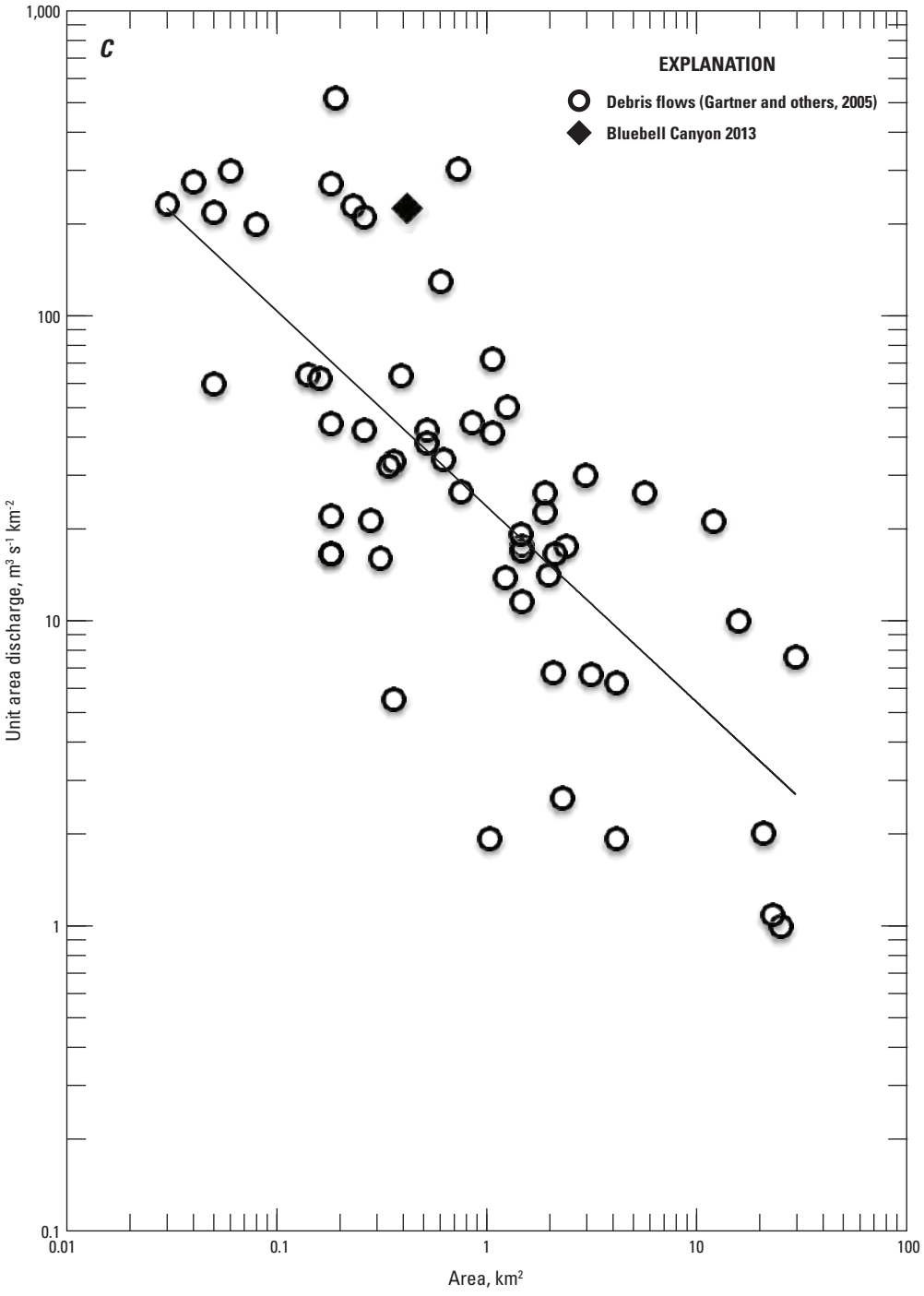

Figure 25. Bluebell Canyon Creek above Mesa Trail Crossing. *A*, View is upstream from cross section 1 (XS1, table 20) on June 6, 2014. *B*, View is upstream of debris deposited downstream from Mesa Trail Crossing. Photograph taken on November 10, 2013. *C*, The Bluebell Canyon Creek debris flow among debris flows generated from other burned areas. [$m^3 s^{-1} km^{-2}$, cubic meter per second per square kilometer; km^2, square kilometer]

Table 20. Summary of indirect discharge measurements for Bluebell Canyon Creek above Mesa Trail Crossing, Boulder County, Colorado.

[ID, cross section identification; XS, cross section; LB, left bank; RB, right bank; HW, high-water mark; SAC, slope-area calculation; stdev, standard deviation; COV, coefficient of variation; m, meter; m^2, square meter; ms^{-1}, meter per second; $m^3 s^{-1}$, cubic meter per second; na, not applicable]

ID	Distance from arbitrary zero (m)	Arbitrary elevation			Hydraulic radius (m)	Depth (m)	Width (m)	Area (m^2)	Mean cross-sectional velocity				Debris flow velocity	Discharge					Debris flow discharge
		LB HW (m)	RB HW (m)	Thalweg (m)					Jarrett ($m\ s^{-1}$)	Cowan ($m\ s^{-1}$)	Empirical ($m\ s^{-1}$)	Critical flow ($m\ s^{-1}$)	Bagnold ($m\ s^{-1}$)	Jarrett ($m^3\ s^{-1}$)	Cowan ($m^3\ s^{-1}$)	Empirical ($m^3\ s^{-1}$)	Critical flow ($m^3\ s^{-1}$)	Ensemble average ($m^3\ s^{-1}$)	Bagnold ($m^3\ s^{-1}$)
XS1	63	106.53	106.95	102.47	1.9	2.3	13.3	30.8	8.7	16.2	8.2	8.2	3.0	267	497	252	254	na	91
XS2	53	105.27	105.25	101.04	1.7	2.2	13.5	29.2	7.6	16.2	7.4	7.4	2.7	222	473	217	216	na	78
XS3	43	104.46	103.15	100.32	1.9	2.3	13.1	30.3	9.7	16.5	9.3	9.2	3.0	293	499	281	279	na	90
XS4	33	102.51	102.57	98.78	2.0	2.5	14.0	35.7	9.3	16.4	9.0	9.0	3.4	331	587	322	320	na	122
XS5	23	101.08	101.36	97.20	2.2	2.7	13.4	36.2	9.8	17.6	9.1	9.1	3.7	354	638	329	331	na	135
XS6	13	98.60	98.60	95.68	1.8	2.1	12.4	26.3	6.8	14.4	6.8	6.5	2.6	178	379	178	171	na	69
XS7	0	97.00	97.67	93.98	1.9	2.1	14.3	30.5	6.9	13.9	6.7	6.6	2.6	210	424	204	200	na	80
												Average		265	500	255	253	318	95
												stdev		65	89	59	61	121	24
												COV		0.25	0.18	0.23	0.24	0.38	0.26

Bear Canyon Creek above Bear Mountain Drive

The indirect peak discharge (12 $m^3 s^{-1}$, tables 1 and 21) was measured on January 7 and 21, 2014. This is an ephemeral stream and extensive vegetation had grown in the channel before the floods (fig. 26). Besides small willows and cottonwood trees on the flood plain and in the channel, there were extensive clumps of multiple stemmed willows or alders (identifying bark and leaves were stripped off by the water and suspended sediment) in the channel. The flood water bent these dense clumps over into compact masses (fig. 26). These clumps were assumed to have little or no water flowing through them but acted like quasi-solid material that obstructed the flow and generated interacting eddies (total n=0.26 $m^{-1/3}$ s; Arcement and Schneider, 1992). For this reason, more water probably flowed over the small flood-plain segments and banks. The different indirect methods estimated that 78–92 percent of the flow was conveyed in the main channel.

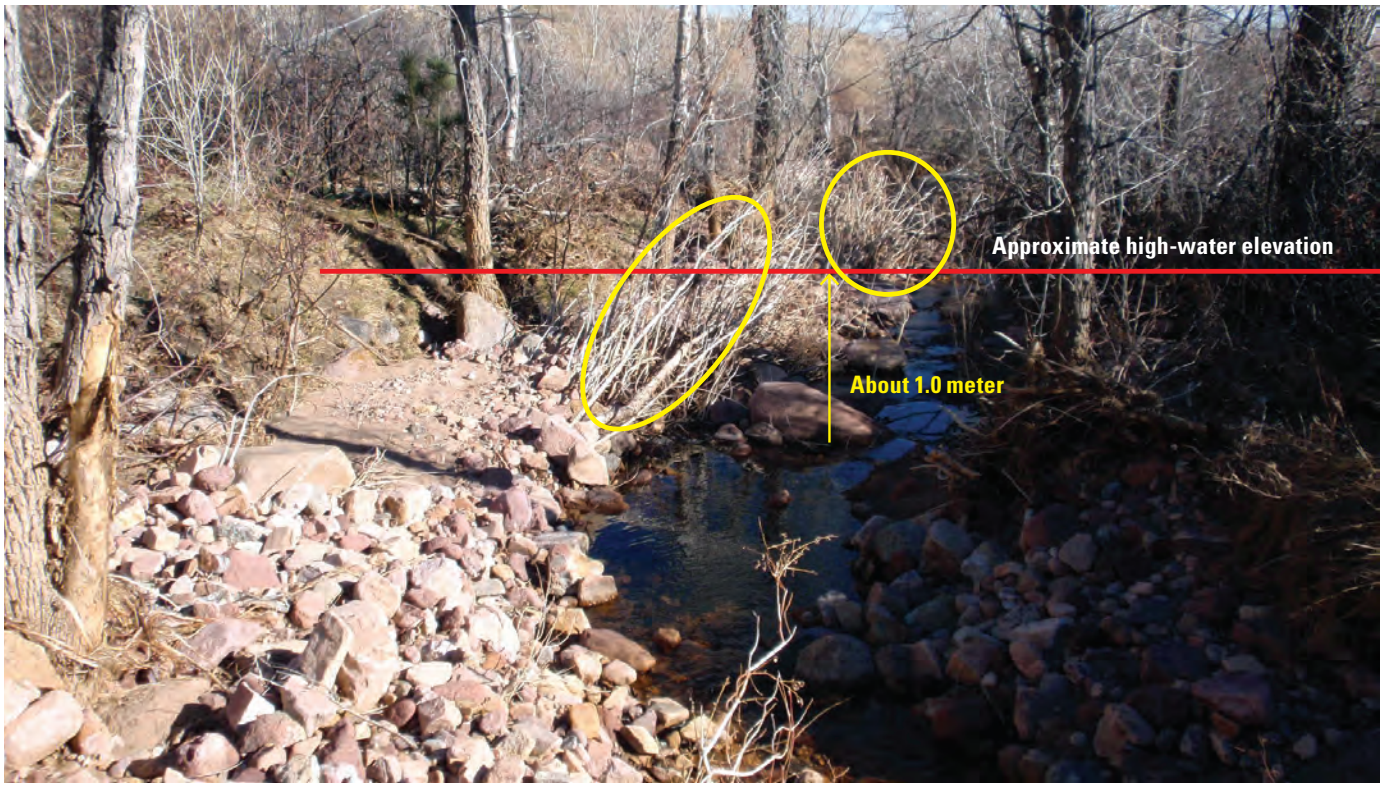

Figure 26. Bear Canyon Creek above Bear Mountain Drive on January 3, 2014. View is downstream from cross section 5 (XS5, table 21). The yellow ellipses indicate examples of clumps of flexible, small diameter (about 0.02 meter) shrubs.

Table 21. Summary of indirect discharge measurements for Bear Canyon Creek above Bear Mountain Drive, Boulder County, Colorado.

[ID, cross section identification; XS, cross section; LB, left bank; RB, right bank; HW, high-water mark; SAC, slope-area calculation; stdev, standard deviation; COV, coefficient of variation; m, meter; m^2, square meter; ms^{-1}, meter per second; $m^3 s^{-1}$, cubic meter per second; na, not applicable]

ID	Distance from arbitrary zero (m)	Arbitrary elevation			Hydraulic radius (m)	Depth (m)	Width (m)	Area (m^2)	Mean cross-sectional velocity				Discharge					
		LB HW (m)	RB HW (m)	Thalweg (m)					Jarrett ($m\ s^{-1}$)	Cowan ($m\ s^{-1}$)	Empirical ($m\ s^{-1}$)	Critical flow ($m\ s^{-1}$)	Jarrett ($m^3\ s^{-1}$)	Cowan ($m^3\ s^{-1}$)	Empirical ($m^3\ s^{-1}$)	Critical flow ($m^3\ s^{-1}$)	SAC[1] ($m^3\ s^{-1}$)	Ensemble average ($m^3\ s^{-1}$)
XS1	73	99.84	99.69	98.57	0.5	0.8	9.8	7.6	1.5	0.8	1.5	2.2	12	6.2	12	17	--	na
XS2	67.5	99.53	99.48	98.09	0.7	0.8	10.5	7.9	1.7	0.9	1.8	2.3	13	6.7	14	18	4.9	na
XS3	60.2	98.84	99.22	97.70	0.6	0.6	12.4	7.8	1.4	0.8	1.4	2.1	11	5.9	11	17	5.2	na
XS4	53.5	98.61	99.12	97.41	0.7	0.8	14.8	12.1	1.9	0.9	2.1	2.6	23	11.4	26	32	5.7	na
XS5	46.7	98.13	98.31	96.86	0.5	0.5	6.7	3.5	3.1	1.5	3.1	4.8	11	5.2	11	17	5.6	na
XS6	41.0	97.78	97.61	96.41	0.7	0.8	7.5	5.7	1.8	0.9	1.9	2.6	10	5.0	11	15	6.4	na
XS7	32.4	97.43	97.32	95.96	0.7	0.8	8.4	6.7	1.9	0.9	2.1	2.7	13	6.0	14	18	6.9	na
XS8	26.5	96.97	97.24	95.72	0.6	0.7	11.4	7.6	1.6	0.8	1.7	2.4	12	6.1	13	18	6.6	na
XS9	20.5	96.88	96.99	95.52	0.7	0.7	11.0	7.9	1.7	0.8	1.8	2.4	14	6.6	14	19	5.7	na
XS10	13.0	96.40	96.40	95.18	0.5	0.6	12.2	7.0	1.4	0.7	1.3	2.1	10	5.0	9	15	5.5	na
XS11	6.0	96.07	96.25	94.39	0.6	0.7	12.3	8.9	1.7	0.9	1.8	2.8	15	7.6	16	25	5.1	na
XS12	0.0	95.92	95.89	94.64	0.7	0.8	11.4	9.0	2.0	0.9	2.0	2.8	18	8.1	18	25	5.2	na
												Average	14	6.6	14	20	[2]5.6	12
												stdev	3.8	1.8	4.6	5.1	0.7	5.8
												COV	0.28	0.26	0.32	0.26	na	0.49

[1]Spread is the percent difference between discharge computed with no expansion loss and discharge computed with full expansion loss, divided by the discharge computed with full expansion loss. Cross sections with spreads >1 are shown by --.

[2]This is the average energy balanced value for the reach given above that had the minimum spread of 0–1 percent.

Discussion

The September 2013 floods were in response to quite different meteorological conditions than floods caused by summer convective storms and annual floods caused by snowmelt. Near saturation conditions prevailed during the September 2013 floods, whereas often dry conditions exist before summer convective storms. For sites within the Colorado Front Range most of the floodflow was conveyed by the main channel (72–98 percent), and flow along the banks and over narrow flood plains was within the uncertainty of the peak discharge measurements. The ensemble average peak discharge correlated best with the critical flow method having a value of R^2=0.99 (which was the same for other methods) but a slope closest to 1.00 (that is, Q[ensemble]=1.01Q[critical flow]) compared to the Cowan (0.92), Jarrett (1.18), empirical (0.75), and slope-area (1.29) methods. This result has an important consequence. By using the critical flow method (which is independent of the flow resistance), the biggest problem in estimating peak discharge (that is determining the flow resistance such as Manning's n) can be avoided.

Relation between Peak Discharge and Rainfall Intensity

Peak discharges produced by infiltration-excess overland flow in response to high-intensity, short-duration summer convective storms depends on the peak rainfall intensity. Commonly, the 30-min peak rainfall intensity correlates with the peak discharge from areas burned by wildfires (Moody and Martin, 2001a; Moody, 2012), but the 30-min interval is probably appropriate (as opposed to some other time interval) because the scale of the burned area is relatively uniform varying from 0.25 to about 25 km^2. Recent work on runoff from burned areas at the hillslope scale (1–100 m^2) indicates that the appropriate rainfall time interval is on the order of 1–10 min (Moody and Ebel, 2014; Moody and Martin, 2015), and work on debris flows from drainage areas ranging from 0.0135–1.37 km^2 indicates a time interval of about 5 min (Kean and others, 2011). The September 2013 floods reported here were generated from drainage areas ranging from 0.0084 to 337 km^2 representing five orders of magnitude. This wide range of drainage area provides data to test the hypothesis that the unit discharge, Q_u, (for saturated-excess overland flow) responds to the average rainfall intensity, I_{Tc} [mm h^{-1}] at a time interval, which is a function of the drainage area and specifically the time-to-concentration, T_c. The linear relation between Q_u and I_{Tc} (fig. 27) had the form as follows:

$$Q_u = 0.26\left(I_{T_c} - 8.6\right); R^2 = 0.69 \qquad (10)$$

This relation depends on T_c; for example, one apparent outlier is the point for Little James Creek above confluence with James Creek (fig. 27; Q_u=9.5 m^3 s^{-1} km^{-2} and I_{Tc}=24.5 mm h^{-1}), which had a peak runoff coefficient of 1.4 assuming that T_c was about 1 h. As mentioned above, if T_c was 10 min, then I_{Tc} would be 44.3 mm h^{-1}, the peak runoff coefficient would be 0.77, and the point representing Little James Creek would fall directly on a new regression line:

$$Q_u = 0.27\left(I_{T_c} - 9.7\right); R^2 = 0.77 \qquad (11)$$

The relation between Q_u and I_{Tc} provides some insight into the rainfall-runoff process for the September 2013 storms. The coefficient 0.26 in equation 10 can be considered as an area-averaged peak runoff coefficient for the September 2013 rain storms in Boulder County. The value 8.6 mm h^{-1} in equation 10 can be considered as a rainfall threshold or more accurately as a soil moisture threshold. Soil moisture controls surface runoff through infiltration rates and the connectivity of subsurface flow. Researchers have determined that a "sharp threshold exists in the relationship between soil water content and runoff coefficient" (Penna and others, 2011, p. 689). Rainfall that exceeds this threshold has been found to produce surface runoff and hydrologically connect riparian zones with adjacent hillslopes through subsurface flow. The result is an abrupt increase in streamflow (Penna and others, 2011). Anecdotal evidence and field observations (during the September 2013 rainfall) of hillslopes runoff (that normally do not respond to rainfall during the year), and the numerous landslides/debris flows on hillslopes support the supposition that hillslopes during the September 2013 storms produced substantial amounts of runoff as a result of the rainfall exceeding a soil moisture threshold.

Comparison with Maximum Worldwide Floods

The September 2013 rainfall was an extreme 1,000-year event for the Colorado Front Range, but the September 2013 floods were not extreme when compared to worldwide floods. The 2013 floods were certainly catastrophic, cutting many mountain highways in numerous places, destroying homes, causing deaths, and costing millions of dollars to rebuild (Lukas, 2013). Two years after the floods the rebuilding was still not complete. The September 2013 floods are about 1–2 orders of magnitude less than the largest worldwide floods (fig. 28). These 54 largest floods were selected based on the criterion of k>5, where k=10([1-(log[Q]-6)/(log[A]-8)]), which is the Francou index (Herschy, 2003).

The scale of the rainfall (≈2,000–5,000 km^2 at the low end of the synoptic range) and the week-long rainfall puts the event within the space-time domain conducive to major regional floods (Hirschboeck, 1988); however, although the rainfall was extreme in terms of amounts, it fell within a narrow southeast-to-northwest trending band across the general west-to-east orientation of the drainage basins along the Colorado Front Range. The rain was not widespread; therefore some of the basins with larger drainage areas were outside the high-accumulation, high-intensity rain band. This is reflected in the wide

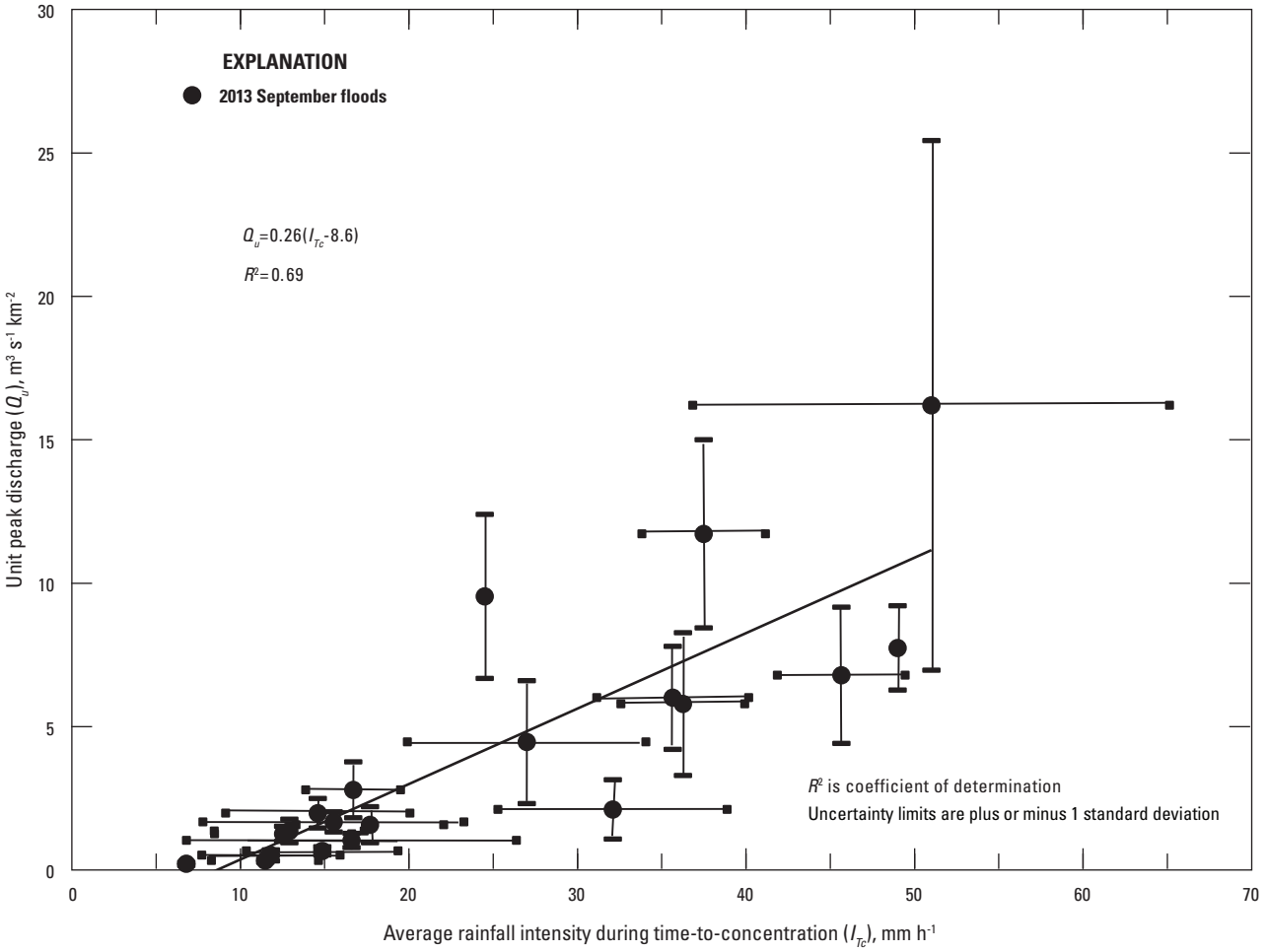

Figure 27. Relation between unit peak discharge and average rainfall intensity during time-to-concentration for the September 2013 floods in the Front Range in Colorado. Only one rain gage was available to compute average rainfall intensity for two sites so that no uncertainty limits are shown. Some uncertainty limits for unit peak discharge are less than the diameter of the solid circle so they do not appear. [$m^3 s^{-1} km^{-2}$, cubic meter per second per square kilometer; $mm\ h^{-1}$, millimeter per hour]

range of peak runoff coefficients (table 1). This contrasting orientation of rainfall and drainage networks probably contributed to the reduction in peak discharge and may explain why the September 2013 floods plot as a different population separated from the worldwide floods. Additionally, the rainfall pattern was stationary, which led to high accumulations; however, often synoptic rainfall that moves down a drainage network can produce substantially larger peak discharges.

Sediment Transport Effects

Estimates of peak discharge based on bedload transport (equation 8) were generally less than the ensemble average. Peak discharges ranged from 2 to 27 percent less than the ensemble average for 12 of the 19 sites (table 22), and for three sites they were essentially the same (plus 4 percent for Left Hand Creek below Nugget Gulch, plus 1 percent for Boulder Creek at mouth of Boulder Canyon, and minus 2 percent for Gregory Creek at Rest Area) and less than the uncertainty of the measurements. The peak discharge estimated with bedload transport probably overestimated the flow relative to the ensemble average for the site Bear Canyon Creek above Bear Mountain Drive because the flow resistance caused by the numerous vegetation clumps was greater than that caused by sediment transport effects.

Estimates of bedload transport rates (1 to 1,600 $kg\ m^{-1} s^{-1}$; table 22) are substantially greater than measured transport rates for nonflooding mountain streams. In general, energy to transport the bedload is extracted from the mean velocity (Wang and Larsen, 1994; Pierson, 2005) causing a decrease in velocity and an apparent increase in flow resistance or Manning's n (values ranged from 0.05 to 0.08 $m^{-1/3}$ s); thus, velocities estimated by using equation 8 in equation 2 were

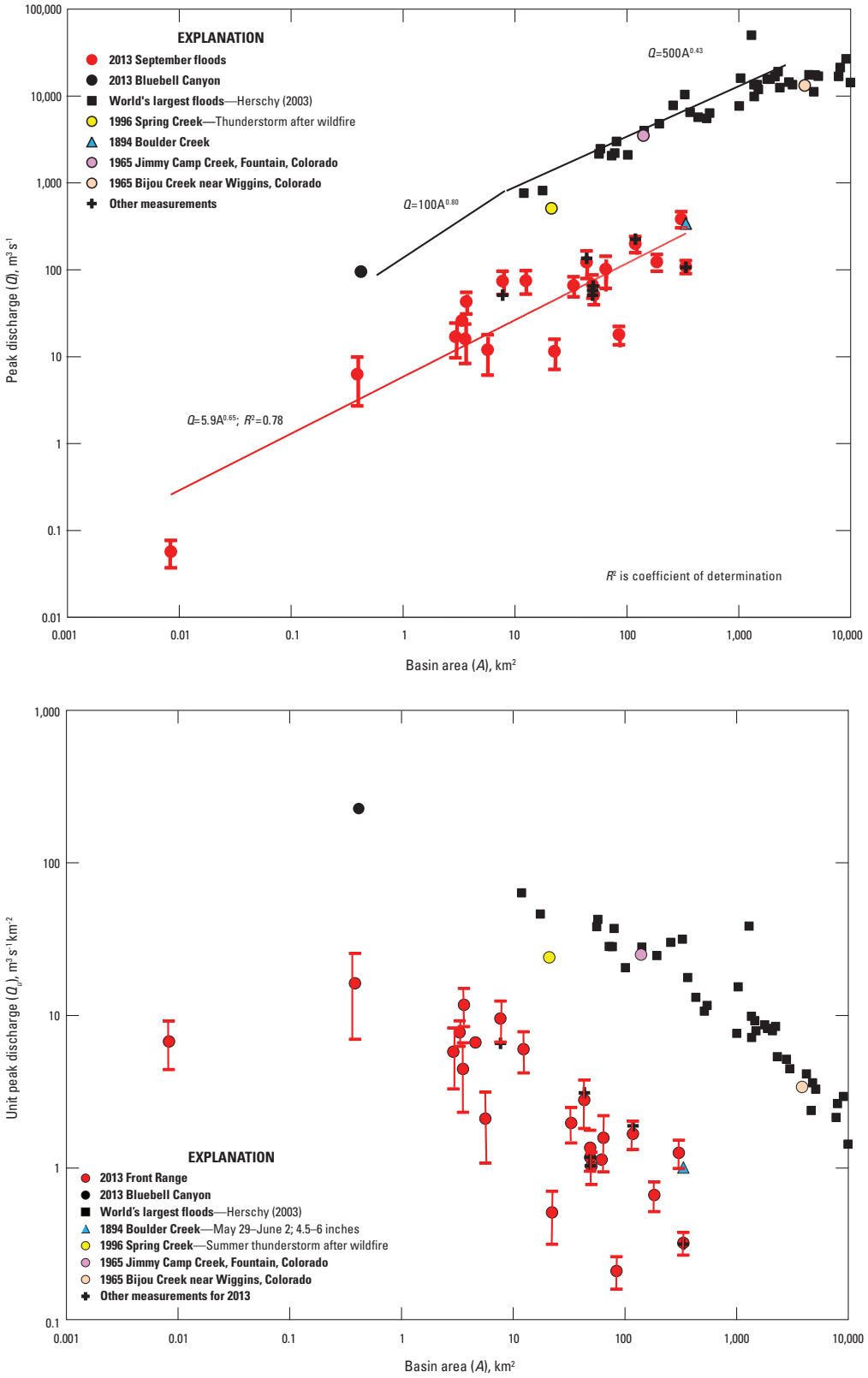

Figure 28. Comparison of peak and unit peak discharges and basin area for the September 2013 floods in the Front Range in Colorado with the world's largest floods and some large floods in Colorado. Uncertain limits are plus or minus one standard deviation of the different methods used to estimate peak discharge. *A*, Comparison of peak discharge and basin area. [$m^3 s^{-1}$, cubic meter per second; km^2, square kilometer] *B*, Comparison of unit peak discharge and basin area. [$m^3 s^{-1} km^{-2}$, cubic meter per second per square kilometer; km^2, square kilometer]

Table 22. Comparison of the peak discharge estimate based on sediment-transport effects with the ensemble average.

[COV, coefficient of variation; $m^3 s^{-1}$, cubic meter per second; kg $m^{-1} s^{-1}$, kilograms per meter per second; %, percent; na, not applicable]

Measurement site name	Peak discharge based on equation (8) + COV (percent) ($m^3 s^{-1}$)	Range of estimated bedload transport (kg $m^{-1} s^{-1}$)	Sediment transport effect (Sediment estimate-Ensemble average)/Ensemble average
	Saint Vrain Basin		
North St. Vrain Creek above Highway 7 Bridge	21 +21%	1–20	0.17
North St. Vrain Creek above Apple Valley Bridge	290 +19%	50–160	-0.25
South St. Vrain Creek above confluence with Middle St. Vrain Creek[1]	60 +16%	30–260	-0.09
South St. Vrain Creek below confluence with Middle St. Vrain Creek	94 +25%	40–200	-0.09
	Left HandBasin		
Little James Creek above confluence with James Creek	54 +11%	110–520	-0.27
James Creek above Jamestown	80 +26%	90–1,600	-0.22
James Creek below Jamestown	109 +15%	90–450	-0.11
Left Hand Creek below Nugget Gulch	54 +31%	180–740	0.04
Left Hand Creek at Buckingham Park	171 +17%	60–380	-0.14
	Boulder Basin		
Fourmile Canyon Creek at 491 Wagonwheel Gap	67 +15%	40–750	-0.11
Twomile Canyon Creek at 215 Linden	33 +22%	240–1,200	0.27
Fourmile Creek above Long Gulch[1]	11 +29%	190–390 20–130	-0.08
Long Gulch above Lorretta-Linda	15 +34%	8–750	-0.06
Loretta-Linda at flume 9-1	6.9 +36%	60–1,300	0.10
Sugarloaf[2]	na	na	na
Fourmile Creek at Logan Mill	60 +30%	30–360	-0.10
Boulder Creek at mouth of Boulder Canyon	110 +12%	50–340	0.01
Gregory Creek below Long Canyon	27 +20%	140–1,300	0.37
Gregory Creek at Rest Area	42 +20%	150–520	-0.02
Bluebell Canyon Creek above Mesa Trail Crossing[3]	na	na	na
Bear Canyon Creek above Bear Mountain Drive	22 +25%	30–460	0.83

[1]Two values are given for above and below the bend in the measurement reach.

[2]The sediment transport estimate was not applicable to this hillslope channel.

[3]The sediment transport estimate was not applicable for this probable debris flow.

frequently more realistic (2.1 to 5.8 m s^{-1}) than those estimated by using the Cowan or Empirical methods. Other contrasting sediment transport effects, however, are possible (Kristin Bunte, Colorado State University, written commun., 2015). At these potential transport rates, the layer of bedload moving along the bed may be thick enough to make a substantial decrease in the flood depth (water depths were estimated after the flood not during the flood) and hence further decrease the peak discharge. At the same time, this moving bed layer may fill in between large roughness elements and effectively "smooth" the bed, thus, reducing the flow resistance and increasing the peak discharge.

Estimates of peak discharge based on bedload transport were most similar to those estimated by the critical flow method. This suggests that bedload transport may be a factor that limits the Froude number to be approximately 1 when sediment is readily available; thus, the critical flow method may implicitly account for the flow resistance caused by sediment transport better than other methods.

Summary

The September 2013 floods were in response to unique meteorological conditions that caused extreme rainfall along the Colorado Front Range. These conditions caused persistent rainfall (about 450 millimeters in 7 days) that saturated the soil and produced a narrow band (about 50 kilometers wide) of high-accumulation, high-intensity rainfall trending southeast to northwest (80–100 kilometers) and oriented nearly perpendicular to the drainage pattern of the Colorado Front Range.

Indirect measurements of the peak discharge were made at 21 sites in the Colorado Front Range of Boulder County, Colorado. The discharge was estimated as the ensemble average of the Cowan, Jarrett, Empirical, Critical flow, and Slope-area methods at 18 sites; as the ensemble average of the Critical flow, Measured "n", Yochum, and Comiti methods at one site; and the Bagnold method was used at one site where evidence indicated that the flood flow was a debris flow. Standard deviation of each ensemble provided an estimate of the uncertainty of the peak discharge except for the debris flow. Because of the extensive evidence of sediment erosion, transport, and deposition, a separate estimate of the peak discharge was made by using a method that estimated the effects of bedload transport on flow resistance (Manning's n).

The time interval for calculating the average peak rainfall intensities was equal to the time-to-concentration for the basin area upstream from each measurement site. Most measurement sites were ungaged or the gaged failed during the floods so complete hydrographs and total flow volumes were not available, and therefore the "peak runoff coefficient" was calculated as the unit peak discharge divided by the average peak rainfall intensity. This metric tends to overestimate the runoff coefficient but provides relative comparisons between measurement sites.

The September 2013 floods were in steep, narrow, and rough mountain channels with drainage areas ranging from 0.0084 to 337 square kilometers and time-to-concentration values from 1.3 to 506 minutes. Mean bed slopes ranged from 0.006 to 0.37, width/depth ratios from 3.4 to 21.0, and the roughness of the bed and bank (D_{84} z-axis) from 105 to 710 millimeters. The ensemble average provided estimates of the peak discharges (0.057–385 cubic meter per second) and the uncertainty of these estimates is best expressed by the coefficient of variation (COV), which ranged from 17 to 57 percent with a mean of 32 percent. Peak discharges estimated by using the sediment transport method were 6 to 27 percent less than values estimated by the ensemble average at 11 of 19 measurement sites. Sediment transport may be a mechanism that limits velocities in these types of mountain streams such that the Froude number fluctuates about 1, which may explain why the critical flow method best correlates with the ensemble average; and therefore, may be the best method to use to estimate the peak discharge in mountain streams similar to those described in this report. However, the use of one method does not provided an estimate of the uncertainty of the peak discharge. Flood plains were either nonexistent or discontinuous, and usually less than the width of the channel. Thus, most of the peak discharge (72–98 percent) was conveyed by the main channel indicating that for these conditions the component of peak discharge over flood plains is less than the uncertainty of the peak discharge and could be ignored, which would expedite the effort required to estimate peak discharges for similar floods in the future.

Peak discharge for the September 2013 floods depended on the drainage area and the rainfall intensity. When the discharge was normalized by the drainage area to produce the unit peak discharge, a linear relation (coefficient of determination [R^2]=0.69) was determined between unit peak discharge and average rainfall intensity, where the slope of the relation represented an area-averaged peak runoff coefficient of 26 percent, and the intercept of the relation (8.6 millimeter per hour) can be thought of as the equivalent average rainfall intensity corresponding to a soil moisture threshold that controls infiltration rates. These unit peak discharges were 1–2 orders of magnitude less than the largest worldwide floods. One possible explanation is that although the rainfall amounts associated with the September 2013 floods were extreme and conducive to major regional floods, the rain fell within a narrow band oriented across the trend of the drainage basins. This reduced the potential magnitude of the peak discharges, so that although the September 2013 rainfall was considered extreme the September 2013 floods were not.

Acknowledgments

Indirect discharge measurement cannot be done alone, and several people helped (Brian Ebel; Ellie Griffin; Jason Kean; Walter Killion; Deborah Martin; Jane Moody; Glenn Patterson; Francis Rengers; James Smith, III; and Jeff Writer).

David Gochis helped to make the measurements during some difficult weather and site conditions. Bob Holmes provided timely assistance that made this report possible. Janis Fulford led me through the art of applying the slope-area calculation (SAC) program, and Mark Smith provided enormous help with interpreting the intricacies of the SAC results. Careful reviews by Eleanor Griffin, Todd Koenig, and Rebekah Davis definitely improved the internal consistency and clarity of this report.

References Cited

Aberle, J., and Smart, G.M., 2003, The influence of roughness structure on flow resistance on steep slopes: Journal of Hydraulic Research, v. 41, no. 3, p. 259–269. [Also available at http://dx.doi.org/10.1080/00221680309499971.]

Ajami, N.K., Duan, Qingyun, Gao, Xiaogang, and Sorooshian, Soroosh, 2006, Multimodel combination techniques for analysis of hydrological simulations—Application to distributed model intercomparison project results: Journal of Hydrometeorology, v. 7, no. 4, p. 755–768. [Also available at http://dx.doi.org/10.1175/JHM519.1.]

Arcement, G.J., Jr., and Schneider, V.R., 1992, Guide for selecting Manning's roughness coefficients for natural channels and flood plains: U.S. Geological Survey Water-Supply Paper 2339, 38 p. [Also available at http://pubs.er.usgs.gov/publication/wsp2339.]

Barnes, H.H., Jr., 1967, Roughness characteristics of natural channels: U.S. Geological Survey Water-Supply Paper 1849, 213 p. [Also available at http://pubs.usgs.gov/wsp/wsp_1849/.]

Bathurst, J.C., 1978, Flow resistance of large-scale roughness: Journal of the Hydraulics Division, v. 104, no. 12, p. 1587–1603.

Bathurst, J.C., 1985, Flow resistance estimation in mountain rivers: Journal of Hydraulic Engineering, v. 111, no. 4, p. 625–643. [Also available at http://dx.doi.org/10.1061/(ASCE)0733-9429(1985)111:4(625).]

Benson, M.A., and Dalrymple, T., 1967, General field and office procedures for indirect measurements: U.S. Geological Survey Techniques of Water-Resources Investigations, book 3, chapter A1, 30 p., http://pubs.er.usgs.gov/publication/twri03A1.

Bilodeau, S.W., Van Buskirk, Donald, and Bilodeau, W.L., 1987, Geology of Boulder, Colorado, U.S.A.: Bulletin of the Association of Engineering Geologists, v. 24, No. 3., p. 293–328.

Birkland, P.W., Shroba, R.R., Burns, S.F., Price, A.B., and Tonkin, P.J., 2003, Integrating soils and geomorphology in mountains—An example from the Front Range of Colorado: Geomorphology, v. 55, p. 329–344.

Bunte, Kristin, 1996, Analyses of the temporal variation of coarse bedload transport and its grain size distribution—Squaw Creek, Montana, USA: U.S. Department of Agriculture, Forest Service, General Technical Report RM–GTR–288, 123 p.

Campbell, Loma, McEwan, Ian, Nikora, Vladimir, Pokrajac, Dubravka, Gallagher, Michael, and Manes, Costantino, 2005, Bed-load effects on hydrodynamics of rough-bed open-channel flows: Journal of Hydraulic Engineering, v. 131, no. 7, p. 576–585. [Also available at http://dx.doi.org/10.1061/(ASCE)0733-9429(2005)131:7(576).]

Capesius, J.P., and Stephens, V.C., 2009, Regional regression equations for estimation of natural streamflow statistics in Colorado: U.S. Geological Survey Scientific Investigations Report 2009–5136, 46 p. [Also available at http://pubs.usgs.gov/sir/2009/5136/.]

Chow, V.T., 1964, Handbook of applied Hydrology: McGraw-Hill Book Company, San Francisco, Chap. 7, 49 p.

Coe, J.A., Kean, J.W., Godt, J.W., Baum, R.L., Jones, E.S., Gochis, D.J., and Anderson, G.S., 2014, New insights into debris-flow hazards from an extraordinary event in the Colorado Front Range: GSA Today, v. 24, no. 10, p. 4–10. [Also available at http://dx.doi.org/10.1130/GSATG214A.1.]

Comiti, Francesco, Mao, Luca, Wilcox, Andrew, Wohl, E.E., and Lenzi, M.A., 2007, Field-derived relationships for flow velocity and resistance in high-gradient streams: Journal of Hydrology, v. 340, no. 1–2, p. 48–62. [Also available at http://dx.doi.org/10.1016/j.jhydrol.2007.03.021.]

Cowan, W.L., 1956, Estimating hydraulic roughness coefficients: Agricultural Engineering, v. 37, p. 472–475.

Douglas, M.W., Maddox, R.A., Howard, K., and Reyes, S., 2004, The North American Monsoon: Reports to the Nation on our Changing Planet, 25 pp. [Available at: http://www.cpc.noaa.gov/products/outreach/Report-to-the-Nation-Monsson_aug04.pdf], NOAA/National Weather Service, Tucson, Arizona.

Ebel, B.A., Moody, J.A., and Martin, D.A., 2012, Hydrologic conditions controlling runoff generation immediately after wildfire: Water Resources Research, v. 48, no. 3, 13 p. [Also available at http://dx.doi.org/10.1029/2011WR011470.]

Ebel, B.A., Rengers, F.K., and Tucker, G.E., 2015, Aspect-dependent soil saturation and insight into debris-flow initiation during extreme rainfall in the Colorado Front Range: Geology, v. 43, no. 8, p. 659–662. [Also available at http://dx.doi.org/10.1130/G36741.1.]

Ferguson, Rob, 2007, Flow resistance equations for gravel- and boulder-bed streams: Water Resources Research, v. 43, no. 5, 12 p. [Also available at http://dx.doi.org/10.1029/2006WR005422.]

Fulford, J.M., 1994, User's guide to SAC, a computer program for computing discharge by slope-area method: U.S. Geological Survey Open-File Report 94–360, 31 p. [Also available at http://pubs.er.usgs.gov/publication/ofr94360.]

Gartner, J.E., Cannon, S. H., Bigio, E.R., Davis, N.K., Parrett, Charles, Pierce, K.L., Rupert, M.G., Thurston, B.L., Trebish, M.J., Garcia, S.P., and Rea, A.H., 2005, Compilation of data relating to the erosive respose of 606 recently-burned basins in the Western U.S.: U.S. Geological Survey Open-File Report 2005–1218. [Also available at http://pubs.usgs.gov/of/2005/1218/.]

Gilcrest, B.R., 1950, Flood routing, chap. X *of* Rouse, Hunter, Engineering hydraulics—Proceedings of the fourth Hydraulic Conference, Iowa Institute of Hydraulic Research, June 12–15, 1949: New York, John Wiley and Sons, Inc., p. 634–710.

Gochis, David, Schumacher, Russ, Friedrich, Katja, Doesken, Nolan, Kelsch, Matt, Sun, Juanzhen, Ikeda, Kyoko, Lindsey, Daniel, Wood, Andy, Dolan, Brenda, Matrosov, Sergey, Newman, Andrew, Mahoney, Kelly, Rutledge, Steven, Johnson, Richard, Kucera, Paul, Kennedy, Pat, Sempere-Torres, Daniel, Steiner, Matthias, Roberts, Rita, Wilson, Jim, Yu, Wei, Chandrasekar, V., Rasmussen, Roy, Anderson, Amanda, and Brown, Barbara, 2014, The great Colorado flood of September 2013: Bulletin of the American Meteorological Society. [Also available at http://dx.doi.org/10.1175/BAMS-D-1300241.1.]

Gomez, Basil, 1991, Bedload transport: Earth-Science Reviews, v. 31, no. 2, p. 89–132. [Also available at http://dx.doi.org/10.1016/0012-8252(91)90017-A.]

Grant, G.E., 1997, Critical flow constrains flow hydraulic in mobile-bed streams—A new hypothesis: Water Resources Research, v. 33, no. 2, p. 349–358. [Also available at http://dx.doi.org/10.1029/96WR03134.]

Griffiths, G.A., 1981, Flow resistance in coarse gravel bed rivers: Journal of the Hydraulics Division, v. 107, no. 7, p. 899–918.

Hansen, W.R., Chronic, John, and Matelock, John, 1978, Climatography of the Front Range urban corridor and vicinity, Colorado: U.S. Geological Survey Professional Paper 1019, 59 p.

Helsel, D.R., and Hirsch, R.M., 2002, Statistical methods in water resources: U.S. Geological Survey Techniques of Water-Resources Investigations, book 4, chap. A3, 522 p.

Herschy, R.W., comp., 2003, World catalogue of maximum observed floods: Wallingford, Oxfordshire, United Kingdom, International Association of Hydrological Sciences, IAHS–AISH Publication 284, 285 p.

Hicks, D.M., and Mason, P.D., 1998, Roughness characteristics of New Zealand rivers: National Institute of Water and Atmospheric Research Ltd., 329 p.

Hirschboeck, K.K., 1988, Flood hydroclimatology, chap. 2 of Baker, V.R., Kochel, R.C., and Patton, P.C., eds., Flood geomorphology: New York, Wiley-Interscience publication, John Wiley and Sons, p. 27–49.

Hungr, O., Morgan, G.C., and Kellerhals, R., 1984, Quantitative analysis of debris torrent hazards for design of remedial measures: Canadian Geotechnical Journal, v. 21, no. 4, p. 663–677. [Also available at http://dx.doi.org/10.1139/t84-073.]

Jarrett, R.D., 1984, Hydraulics of high-gradient streams: Journal of Hydraulic Engineering, v. 110, no. 11, p. 1519–1539. [Also available at http://dx.doi.org/10.1061/(ASCE)0733-9429(1984)110:11(1519).]

Jarrett, R.D., 1987, Errors in slope-area computations of peak discharges in mountain streams: Journal of Hydrology, v. 96, no. 1–4, p. 53–67. [Also available at http://dx.doi.org/10.1016/0022-1694(87)90143-0.]

Jarrett, R.D., and Costa, J.E., 2006, 1976 Big Thompson Flood, Colorado—Thirty years later: U.S. Geological Survey Fact Sheet 2006–3095, 5 p.

Judd, H.E., and Peterson, D.F., 1969, Hydraulics of large bed element channels: Logan, Utah, Utah State University, College of Engineering, Utah Water Research Laboratory, Paper 285, 115 p. [Also available at http://digitalcommons.usu.edu/water_rep/285/.]

Kean, J.W., and Smith, J.D., 2010, Calculation of stage-discharge relations for gravel bedded channels: Journal of Geophysical Research, v. 115, no. F3, 15 p. [Also available at http://dx.doi.org/10.1029/2009JF001398.]

Kean, J.W., Staley, D.M., and Cannon, S.H., 2011, In situ measurements of post-fire debris flows in southern California—Comparisons of the timing and magnitude of 24 debris-flow events with rainfall and soil moisture conditions: Journal of Geophysical Research, v. 116, no. F4, 21 p. [Also available at http://dx.doi.org/10.1029/2011JF002005.]

Kilpatrick, F.A. and Schneider, V.R., 1983, Use of flumes in measuring discharge: U.S. Geological Survey Techniques of Water-Resources Investigations, book 3, chap. A14, 46 p. [Also available at http://pubs.usgs.gov/twri/twri3-a14/.]

Kinner, D.A., and Moody, J.A., 2008, Infiltration and runoff measurements of steep burned hillslopes using a rainfall simulator with variable rain intensities: U.S. Geological Survey Scientific Investigations Report 2007–5211, 64 p. [Also available at http://pubs.usgs.gov/sir/2007/5211/.]

Limerinos, J.T., 1970, Determination of the Manning coefficient from measured bed roughness in natural channels: U.S. Geological Survey Water-Supply Paper 1898–B, 47 p. [Also available at http://pubs.er.usgs.gov/publication/wsp1898B.]

Lukas, Jeff, 2013, September 2013 front range flooding event—Weather, hydrologic impacts, context of a changing climate, implications: Fort Collins, Colo., Colorado Water Institute, Colorado State University.

Luque, R.F. and Beek, R. van, 1976, Erosion and transport of bed-load sediment, Journal of Hydraulic Research, v. 14, no. 2, p. 127–144. [Also available at http://dx.doi.org/10.1080/00221687609499677.]

Manzi, A., 2013, A Thousand-year Rain, The Histoci Flood of 2013 in Boulder and Larimer Counties, Prairie Mountain Publishing, ISBN 978-1-59725-485-4, 160 p.

Marchard, J.P., Jarrett, R.D., and Jones, L.L, 1984, Velocity profile, water-surface slope, and bed-material size for selected streams in Colorado: U.S. Geological Survey Open-File Report 84–733, 80 p. [Also available at http://pubs.er.usgs.gov/publication/ofr84733.]

Milhous, R.T., 1973, Sediment transport in a gravel-bottomed stream: Oregon State University, Ph.D. thesis, 214 p. with appendixes. [Also available at http://hdl.handle.net/1957/9364.]

Moody, J.A., 2012, An analytical method for predicting post-wildfire peak discharges: U.S. Geological Survey Scientific Investigations Report 2011–5236, 36 p. [Also available at http://pubs.usgs.gov/sir/2011/5236/.]

Moody, J.A., and Ebel, B.A., 2014, Infiltration and runoff generation processes in fire-affected soils: Hydrological Processes, v. 28, no. 9, p. 3432–3453. [Also available at http://dx.doi.org/10.1002/hyp.9857.]

Moody, J.A., and Martin, D.A., 2001a, Post-fire, rainfall intensity-peak discharge relations for three mountainous watersheds in the western USA: Hydrological Processes, v. 15, no. 15, p. 2981–2993. [Also available at http://dx.doi.org/10.1002/hyp.386.]

Moody, J.A. and Martin, D.A., 2001b, Hydrologic and sedimentologic response of two burned watersheds in Colorado: U.S. Geological Survey Water-Resources Investigation Report 2001–4122, 138 p. [Also available at http://pubs.er.usgs.gov/publication/wri014122.]

Moody, J.A. and Martin, R.G., 2015, Measurement of the initiation of post-wildfire runoff during rainstorms using in situ overland flow detectors: Earth Surface Processes and Landforms, v. 40, no. 8, p. 1043–1065. [Also available at http://dx.doi.org/10.1002/esp.3704.]

Moody, J.A., and Meade, R.H., 1990, Channel changes at cross sections of the Powder River between Moorhead and Broadus, Montana, 1975–88: U.S. Geological Survey Open-File Report 89–407, 252 p. [Also available at http://wwwbrr.cr.usgs.gov/projects/GEOMORPH_Powder_River/references/Moody_1990_OFR89-407DataReport_1.pdf.]

Moreland, D.C., and Moreland, R.E., 1975, Soil survey of the Boulder County area, Colorado: U.S. Department of Agriculture, Soil Conservation Service, Colorado Agriculture Experiment Station, 86 pp.

National Oceanic and Atmospheric Administration, 2013, Exceedance probability analysis for the Colorado flood event, 9–16 September 2013: Silver Spring, Md., National Oceanic and Atmospheric Administration, National Weather Service, Hydrometeorological Design Studies Center, 5 p. [Also available at http://www.nws.noaa.gov/oh/hdsc/aep_storm_analysis/8_Colorado_2013.pdf.]

Natural Resources Conservation Service, 2010, Time to concentration, chap. 15 *of* Natural Resources Conservation Service, Part 630 hydrology, national engineering handbook: U.S. Department of Agriculture, 18 p. with appendixes. [Also available at http://www.wcc.nrcs.usda.gov/ftpref/wntsc/H&H/NEHhydrology/ch15.pdf.]

Penna, Daniele, Tromp-van Meerveld, H.J., Gobbi, Alerto, Borga, Marco, and Fontana, G.D., 2011, The influence of soil moisture on threshold runoff generation processes in an alpine headwater catchment: Hydrology and Earth System Sciences, v. 15, p. 689–702. [Also available at http://dx.doi.org/10.5194/hess-15-689-2011.]

Pierson, T.C., 2005, Hyperconcentrated flow—Transitional process between water flow and debris flow, chap. 8 *of* Jakob, Matthias, and Hungr, Oldrich, eds., Debris-flow hazards and related phenomena: Praxis Publishing Ltd., Springer Berlin Heidelberg, p. 159–202. [Also available at http://dx.doi.org/10.1007/3-540-27129-5_8.]

Pitlick, John, 1992, Flow resistance under conditions of intense gravel transport: Water Resources Research, v. 28, no. 3, p. 891–903. [Also available at http://dx.doi.org/10.1029/91WR02932.]

Prochaska, A.B., Santi, P.M., Higgins, J.D., and Cannon, S.H., 2008, A study of methods to estimate debris flow velocity: Landslides, v. 5, no. 4, p. 431–444. [Also available at http://dx.doi.org/10.1007/s10346-008-0137-0.]

Rantz, S.E. and others, 1982, Measurement and computation of streamflow: Volume 1, Measurement of state and Discharge: U.S. Geological Survey Water-Supply Paper 2175, 284 pages.

Ritsch, M., Hanna, B., and Malers, K., 2013, September 2013 Flood peak discharge estimates along Fourmile Creek: Technical Memorandum, Water and Earth Technologies, Inc., 11 p.

Ryan, S.E., and Emmett, W.W., 2002, The nature of flow and sediment movement in Little Granite Creek near Bondurant, Wyoming: U.S. Department of Agriculture, Forest Service, Rocky Mountain Research Station, General Technical Report RMRS–GTR–90, 48 p. [Also available at http://www.treesearch.fs.fed.us/pubs/21450.]

Smart, G.M., 1984, Sediment transport formula for steep channels: Journal of Hydraulic Engineering, v. 110, no. 3, p. 267–275. [Also available at http://dx.doi.org/10.1061/(ASCE)0733-9429(1984)110:3(267).]

Smith, J.D., and McLean, S.R., 1977, Spatially averaged flow over a wavy surface: Journal of Geophysical Research, v. 82, no. 12, p. 1735–1746. [Also available at http://dx.doi.org/10.1029/JC082i012p01735.]

Wang, Zhaoyin, and Larsen, Peter, 1994, Turbulent structure of water and clay suspensions with bed load: Journal of Hydraulic Engineering, v. 120, no. 5, p. 577–600. [Also available at http://dx.doi.org/10.1061/(ASCE)0733-9429(1994)120:5(577).]

Wilcox, A.C., Nelson, J.M., and Wohl, E.E., 2006, Flow resistance dynamics in step-pool channels—2. Partitioning between grain, spill, and woody debris resistance: Water Resources Research, v. 42, no. 5, 14 p. [Also available at http://dx.doi.org/10.1029/2005WR004278.]

Woodward, D.E., Hawkins, R.H., Jiang, Ruiyun, Hjelmfelt, A.T., Jr., and Mullem, J.A. van, 2003, Runoff curve number method—Examination of the initial abstraction ratio, *in* Bizier, Paul, and DeBarry, Paul, eds., World Water and Environmental Resources Congress 2003: World Water and Environmental Resources Congress, Philadelphia, Pa., June 23–26, 2003 [Proceedings], p. 1–10. [Also available at http://dx.doi.org/10.1061/40685(2003)308.]

Wright Water Engineers, 2014, Rainfall-runoff analysis for September 2013 flood in the City of Boulder, Colorado: Denver, Colo., Wright Water Engineers, Inc., 54 p. with appendixes. [Also available at https://www-static.bouldercolorado.gov/docs/rainfall-runoff-analysis-september-2013-flood-boulder-colorado-1-201411180919.pdf.]

Yager, E.M., Kirchner, J.W., and Dietrich, W.E., 2007, Calculating bed load transport in steep boulder bed channels: Water Resources Research, v. 43, no. 7, 24 p. [Also available at http://dx.doi.org/10.1029/2006WR005432.]

Yochum, S.E., and Bledsoe, B.P., 2010, Flow resistance estimation in high-gradient streams: Federal Interagency Hydrologic Modeling Conference, 4th, Las Vegas, Nevada, June 27–July 1, 2010, 12 p. [Also available at http://acwi.gov/sos/pubs/2ndJFIC/Contents/5E_Yochum_01_04_10_2_.pdf.]

Yochum, S.E., Bledsoe, B.P., David, G.C.L., and Wohl, E.E., 2012, Velocity prediction in high-gradient channels*:* Journal of Hydrology, v. 424–425, p. 84–98. [Also available at http://dx.doi.org/10.1016/j.jhydrol.2011.12.031.]

Yochum, S.E., and Moore, D.S., 2013, Colorado front range flood of 2013—Peak flow estimates at selected mountain stream locations: U.S. Department of Agriculture, Natural Resources Conservation Service, 38 p. [Also available at http://dx.doi.org/10.13140/2.1.2593.0242.]

Zhang, Guaung-hui, Luo, Rong-ting, Cao, Ying, Shen, Rui-chang, and Zhang, X.C., 2010, Impacts of sediment load on Manning coefficient in supercritical shallow flow on steep slopes: Hydrological Processes, v. 24, no. 26, p. 3909–3914. [Also available at http://dx.doi.org/10.1002/hyp.7892.]

Publishing support provided by:
Rolla Publishing Service Centers

For more information concerning this publication, contact:
Chief, USGS Office of Surface Water
415 National Center
12201 Sunrise Valley Drive
Reston, VA 20192
(703) 648-5301

Or visit the Office of Surface Water Web site at:
http://water.usgs.gov/osw/

USGS

Moody— **Estimates of Peak Discharge for 21 Sites in the Front Range in Colorado in Response to Extreme Rainfall in September 2013**—SIR 2016–5003

ISSN 2328-0328 (online)
http://dx.doi.org/10.3133/sir20165003